# Clouds and the Earth's Radiant Energy System (CERES)

## Data Management System

## DRAFT ES-8 Collection Guide

## Release 3
## Version 4


**Primary Authors**

*Lee-hwa Chang, John L. Robbins*

Science Applications International Corporation (SAIC)
One Enterprise Parkway, Suite 300
Hampton, VA 23666-5845

*Richard N. Green, James F. Kibler*

NASA Langley Research Center
Radiation and Aerosols Branch
Atmospheric Sciences Competency
Building 1250
21 Langley Boulevard
Hampton, VA 23681-2199



January 2003

# Document Revision Record

The Document Revision Record contains information pertaining to approved document changes. The table lists the date the Software Configuration Change Request (SCCR) was approved, the Release and Version Number, the SCCR number, a short description of the revision, and the revised sections. The document authors are listed on the cover. The Head of the CERES Data Management Team approves or disapproves the requested changes based on recommendations of the Configuration Control Board.

Document Revision Record

| SCCR Approval Date | Release/ Version Number | SCCR Number | Description of Revision | Section(s) Affected |
|---|---|---|---|---|
| 01/10/01 | R3V3 | 236 | • Added maximum file size with HDF compression to the ES-8 Product Summary Table.<br>• Changed all references to number of records from 13091 to 13092.<br>• Switched the first and second dimensions of the SDS Elements so that the first dimension reflects the number of 6.6-second records contained in the data-day.<br>• Updated format to comply with standards. | 5.0<br>5.0, 5.2, 5.3, & 15.0<br>5.2<br>All |
| 07/03/02 | R3V4 | 369 | • Renamed EOS-PM to Aqua.<br>• Renamed DAAC to ASDC.<br>• The launch and data start date for the Aqua spacecraft was supplied.<br>• ES-8 Vdata, ES8-V21 (Spectral Response Functions), definition was added.<br>• Range for LW TOA flux was changed to 50 .. 450.<br>• Added ES-8 Spectral Response Functions Vdata.<br>• Corrected ES8-V19 and ES8-V20 parameter names to reflect “at observation”.<br>• Term-20, Spectral Correction, was added.<br>• Acronym, EOS PM, was added.<br>• Note-6, Spectral Correction Algorithm, was added.<br>• Detector Time Constants for FM3 and FM4 were added.<br>• Updated format to comply with standards. | All<br>All<br>Table 4-2<br>4.3.1<br>Table 5-3<br>Table 5-4<br>Table 5-4<br>15.0<br>16.1<br>8.0<br>Table 8-2<br>All |
| 07/03/02 | R3V4 | 369 | • The CERES Top Level Data Flow Diagram was modified (5/29/03). | 1.3 |

# Preface

The Clouds and the Earth's Radiant Energy System (CERES) Data Management System supports the data processing needs of the CERES Science Team research to increase understanding of the Earth's climate and radiant environment. The CERES Data Management Team works with the CERES Science Team to develop the software necessary to implement the science algorithms. This software, being developed to operate at the Langley Atmospheric Sciences Data Center (ASDC), produces an extensive set of science data products.

The Data Management System consists of 12 subsystems; each subsystem represents one or more stand-alone executable programs. Each subsystem executes when all of its required input data sets are available and produces one or more archival science products.

This Collection Guide is intended to give an overview of the science product along with definitions of each of the parameters included within the product. The document has been reviewed by the CERES Working Group teams responsible for producing the product and by the Working Group Teams who use the product.

Acknowledgment is given to Tammy O. Ayers and Thanh Duong of Science Applications International Corporation (SAIC) for their support in the preparation of this document.

# TABLE OF CONTENTS

Section Page

Preface . . . iii
Summary . . . 1
1.0 Collection Overview . . . 1
1.1 Collection Identification . . . 1
1.2 Collection Introduction . . . 2
1.3 Objective/Purpose . . . 2
1.4 Summary of Parameters . . . 5
1.5 Discussion . . . 5
1.6 Related Collections . . . 5
2.0 Investigators . . . 6
2.1 Title of Investigation . . . 6
2.2 Contact Information . . . 6
3.0 Origination . . . 7
4.0 Data Description . . . 8
4.1 Spatial Characteristics . . . 8
4.1.1 Spatial Coverage . . . 8
4.1.2 Spatial Resolution . . . 8
4.2 Temporal Characteristics . . . 8
4.2.1 Temporal Coverage . . . 8
4.2.2 Temporal Resolution . . . 9
4.3 Parameter Definitions . . . 9
4.3.1 ES-8 Vdata . . . 9
4.3.2 ES-8 Scientific Data Definitions . . . 13
4.4 Fill Values . . . 28
4.5 Sample Data File . . . 28
5.0 Data Organization . . . 29
5.1 Data Granularity . . . 30
5.2 ES-8 HDF Scientific Data Sets (SDS) . . . 30
5.3 ES-8 HDF Vertex Data (Vdata) . . . 31
5.4 ES-8 Metadata . . . 32
6.0 Theory of Measurements and Data Manipulations . . . 33
6.1 Theory of Measurements . . . 33
6.2 Data Processing Sequence . . . 33
6.3 Special Corrections/Adjustments . . . 33
7.0 Errors . . . 34

# TABLE OF CONTENTS

Section Page

7.1 Quality Assessment . . . . . 34
7.2 Data Validation by Source . . . . . 34
8.0 Notes . . . . . 35
Note-1 Conversion of Julian Date to Calendar Date . . . . . 35
Note-2 Colatitude and Longitude of Nadir . . . . . 38
Note-3 CERES Point Spread Function . . . . . 39
Note-4 Definition of Angular Distribution Models (ADM) . . . . . 44
Note-5 Maximum Likelihood Estimator (MLE) of Scene Type . . . . . 45
Note-6 Spectral Correction Algorithm . . . . . 46
9.0 Application of the Data Set . . . . . 48
10.0 Future Modifications and Plans . . . . . 48
11.0 Software Description . . . . . 48
12.0 Contact Data Center/Obtain Data . . . . . 48
13.0 Output Products and Availability . . . . . 48
14.0 References . . . . . 49
15.0 Glossary of Terms . . . . . 50
16.0 Acronyms and Units . . . . . 54
16.1 CERES Acronyms . . . . . 54
16.2 CERES Units . . . . . 56
17.0 Document Information . . . . . 58
17.1 Document Creation Date - May 15, 1998 . . . . . 58
17.2 Document Review Date - . . . . . 58
17.3 Document Revision Date . . . . . 58
17.4 Document ID . . . . . 58
17.5 Citation . . . . . 58
17.6 Redistribution of Data . . . . . 58
17.7 Document Curator . . . . . 58
18.0 Index . . . . . 59
APPENDIX A CERES Metadata . . . . . A-1

# LIST OF TABLES

Table Page

Table 3-1. CERES Instruments . . . . . 7
Table 4-1. ES-8 Spatial Coverage . . . . . 8
Table 4-2. CERES Temporal Coverage . . . . . 8
Table 4-3. CERES Orbit Characteristics . . . . . 9
Table 4-4. ERBE Scene Types . . . . . 20
Table 4-5. Bit Order for Radiometric and FOV Quality Flags . . . . . 21
Table 4-6. Scanner Operations Flag Word 1 (of 3) . . . . . 22
Table 4-7. Scanner Operations Flag Word 2 (of 3) . . . . . 23
Table 4-8. Scanner Operations Flag Word 3 (of 3) . . . . . 24
Table 4-9. CERES Fill Values . . . . . 28
Table 5-1. ES-8 Product Summary. . . . . 29
Table 5-2. ES-8 Product Specific Metadata . . . . . 29
Table 5-3. ES-8 SDS Summary (1 of 2) . . . . . 30
Table 5-4. ES-8 Vdata Summary (1 of 2) . . . . . 31
Table 8-1. Julian Day Number . . . . . 37
Table 8-2. Detector Time Constant (t seconds) . . . . . 41
Table A-1. CERES Baseline Header Metadata (1 of 2) . . . . . A-1
Table A-2. CERES_metadata Vdata . . . . . A-3

# LIST OF FIGURES

Figure Page

Figure 1-1. CERES Top Level Data Flow Diagram . . . . . 4
Figure 4-1. Colatitude and Longitude . . . . . 12
Figure 4-2. Viewing Angles at TOA . . . . . 16
Figure 8-1. Scanner Footprint Geometry. . . . . 39
Figure 8-2. Optical FOV . . . . . 40
Figure 8-3. TRMM Angular Bin Weights . . . . . 43
Figure 8-4. ERBE Scene Identification Algorithm . . . . . 45
Figure 8-5. CERES_TRMM Spectral Response . . . . . 47
Figure 15-1. Cone Angle . . . . . 50
Figure 15-2. Ellipsoidal Model . . . . . 50
Figure 15-3. Normal and short Earth scan profiles for instrument on TRMM platform. . . . . 52

# Clouds and the Earth's Radiant Energy System (CERES) ES-8 Collection Guide

## Summary

CERES is a key component of the EOS program. The CERES instrument provides radiometric measurements of the Earth's atmosphere from three broadband channels: a shortwave channel (0.3 - 5 µm), a total channel (0.3 - 200 µm), and an infrared window channel (8 - 12 µm). The CERES instruments are improved models of the ERBE scanner instruments, which operated from 1984 through 1990 on NASA's ERBS and on NOAA's operational weather satellites, NOAA-9 and NOAA-10. The strategy of flying instruments on Sun-synchronous, polar orbiting satellites, such as NOAA-9 and NOAA-10, simultaneously with instruments on satellites that have precessing orbits in lower inclinations, such as ERBS, was successfully developed in ERBE to reduce time sampling errors. CERES continues that strategy by flying instruments on the polar orbiting EOS platforms simultaneously with an instrument on the TRMM spacecraft, which has an orbital inclination of 35 degrees. The TRMM satellite carries one CERES instrument while the Terra and Aqua EOS satellites carry two CERES instruments, one operating in a FAPS mode for continuous Earth sampling and the other operating in a RAPS mode for improved angular sampling.

To preserve historical continuity, some parts of the CERES data reduction use algorithms identical with the algorithms used in ERBE. At the same time, many of the algorithms on CERES are new. To reduce the uncertainty in data interpretation and to improve the consistency between the cloud parameters and the radiation fields, CERES includes cloud imager data and other atmospheric parameters. The CERES investigation is designed to monitor the top-of-atmosphere radiation budget as defined by ERBE, to define the physical properties of clouds, to define the surface radiation budget, and to determine the divergence of energy throughout the atmosphere. The CERES DMS produces products which support research to increase understanding of the Earth's climate and radiant environment.

The ES-8 archival data product was created as an HDF-EOS (See Reference 1) swath data structure and contains a 24-hour, single-satellite, instantaneous view of scanner fluxes at the TOA (See Term-22) reduced from spacecraft altitude unfiltered radiances using the ERBE scanner Inversion algorithms and the ERBE SW and LW ADMs. The ES-8 also includes the TOT, SW, and WN channel radiometric data; SW, LW, and WN unfiltered radiance values; and the ERBE scene identification for each measurement. These data are organized according to the CERES 3.3-second scan into 6.6-second records. As long as there is one valid scanner measurement within a record, the ES-8 record will be generated.

## 1.0 Collection Overview

## 1.1 Collection Identification

The ES-8 filename is

CER_ ES8_Sampling-Strategy_Production-Strategy_XXXXXX.YYYYMMDD where

| | |
|---|---|
| CER | Investigation designation for CERES, |
| ES8 | Product identification for the primary science data product (external distribution), |
| Sampling-Strategy | Platform, instrument, and imager (e.g., TRMM-PFM-VIRS), |
| Production-Strategy | Edition or campaign (e.g., At-launch, ValidationR1, Edition1), |
| XXXXXX | Configuration code for file and software version management, |
| YYYY | 4-digit integer defining data acquisition year, |
| MM | 2-digit integer defining data acquisition month, and |
| DD | 2-digit integer defining the data acquisition day. |

## 1.2 Collection Introduction

The ES-8 data product is a Level-2 archival product that contains a 24-hour, single-satellite, single-instrument, instantaneous view of scanner fluxes at the TOA reduced from spacecraft altitude unfiltered radiances using the ERBE scanner Inversion algorithms and the ERBE SW and LW ADMs.

## 1.3 Objective/Purpose

The overall science objectives of the CERES investigation are

1. For climate change research, provide a continuation of the ERBE radiative fluxes at the TOA that are analyzed using the same techniques used with existing ERBE data.
2. Double the accuracy of estimates of radiative fluxes at the TOA and the Earth's surface from existing ERBE data.
3. Provide the first long-term global estimates of the radiative fluxes within the Earth's atmosphere.
4. Provide cloud property estimates which are consistent with the radiative fluxes from surface to TOA.

The CERES DMS is a software management and processing system which processes CERES instrument measurements and associated engineering data to produce archival science and other data products. The DMS is executed at the LaRC ASDC, which is also responsible for distributing the data products. A high-level view of the CERES DMS is illustrated by the CERES Top Level Data Flow Diagram shown in Figure 1-1.

Circles in the diagram represent algorithm processes called subsystems, which are a logical collection of algorithms that together convert input products into output products. Boxes represent archival products. Two parallel lines represent data stores which are designated as nonarchival or temporary data products. Boxes or data stores with arrows entering a circle are input sources for the subsystem, while boxes or data stores with arrows exiting the circles are output products.

As shown in Figure 1-1, the ES-8 product is generated by the CERES ERBE-like Inversion Subsystem (Subsystem 2.0). The input to Subsystem 2.0 is actually the preES-8, a daily file which is generated by an Instrument Subsystem postprocessing program and contains a subset of BDS parameters.

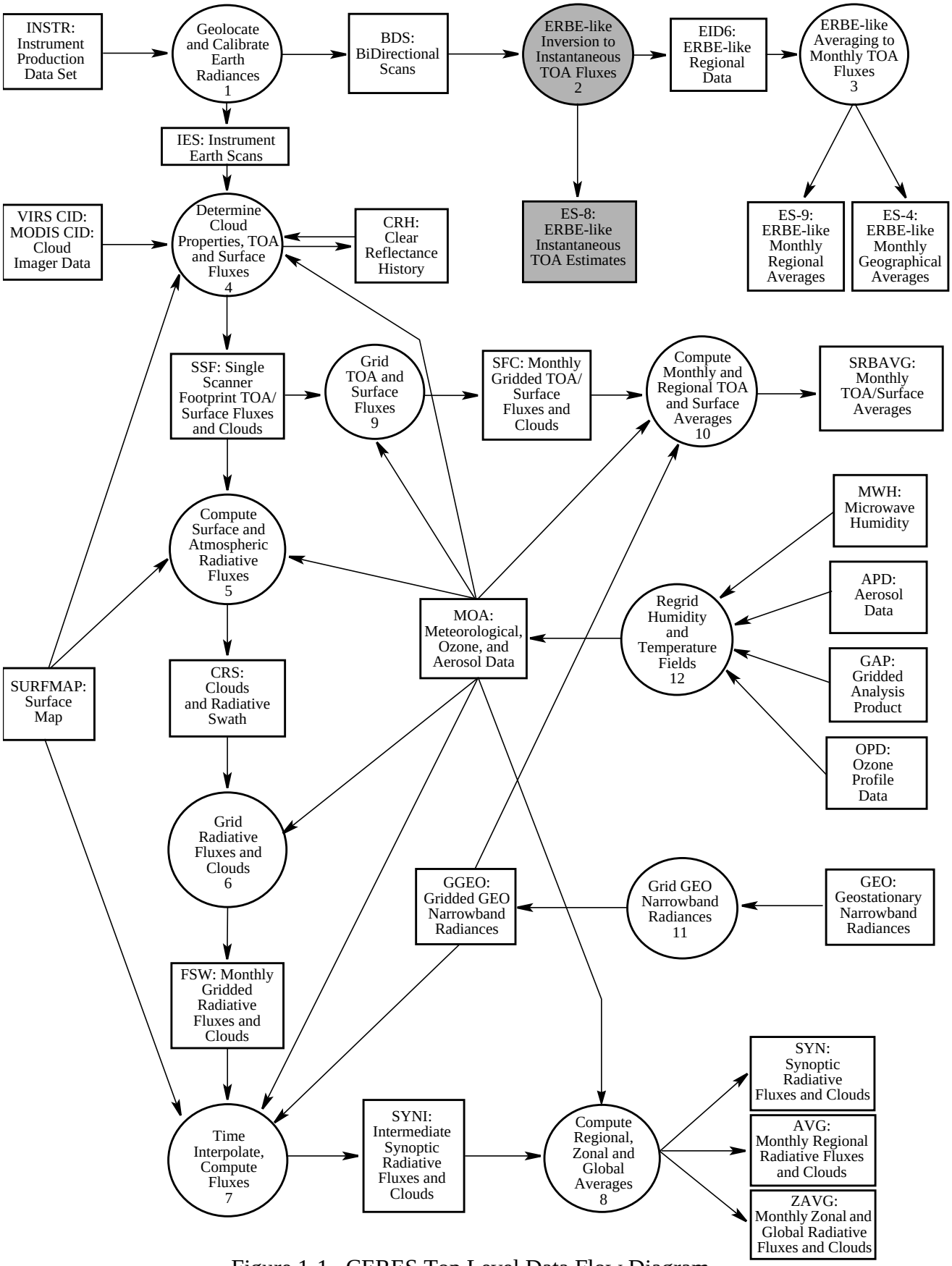


Modified Date: May 2003

Figure 1-1. CERES Top Level Data Flow Diagram

## 1.4 Summary of Parameters

The ES-8 contains the following kinds of information:

1. Scan-level Data (Vdata Structures)

   a) Time of Observation (Julian date and time)
   b) Earth-Sun distance
   c) Satellite position and velocity and Sun position

2. Measurement-level Data (SDSs)

   a) Instrument field-of-view (colatitude and longitude)
   b) Radiometric data (total, shortwave, and window channels)
   c) Satellite and Sun geometry (viewing zenith, solar zenith, and relative azimuth)
   d) Unfiltered radiances (shortwave, longwave, and window)
   e) TOA fluxes (shortwave and longwave)
   f) ERBE scene identification

| | | |
|---|---|---|
| ( 1) clear ocean | ( 5) clear coastal | ( 9) mostly cloudy ocean |
| ( 2) clear land | ( 6) partly cloudy ocean | (10) mostly cloudy land-desert |
| ( 3) clear snow | ( 7) partly cloudy land-desert | (11) mostly cloudy coastal |
| ( 4) clear desert | ( 8) partly cloudy coastal | (12) overcast |

## 1.5 Discussion

Satellite altitude data from the Instrument Subsystem is processed by the ERBE-like Inversion Subsystem to provide estimates of the radiant flux at the TOA. This inversion process is dependent on several factors, including Earth surface features, the extent of cloudiness, and the relative geometry of the satellite, the Sun, and the measurement FOV. Each radiometric measurement is spectrally corrected (See Term-20) to give an unfiltered measurement. The observed scene is determined by the ERBE scene identification algorithm based on these unfiltered measurements using ADMs and statistics provided by the Science Team. Estimates of the radiant flux at the TOA are computed based on the scene information, geometrical considerations, and the unfiltered measurements.

## 1.6 Related Collections

The CERES DMS produces science data products, or collections, for use by the CERES Science Team, the Data Management Team, and for archival at the Langley ASDC. A complete list of collections may be found in the CERES DPC (See Reference 2).

## 2.0 Investigators

Dr. Bruce A. Wielicki, CERES Principal Investigator
E-mail: B.A.Wielicki@LaRC.NASA.Gov
Telephone: (757) 864-5683
FAX: (757) 864-7996
Mail Stop 420
Atmospheric Sciences Competency
Building 1250
21 Langley Boulevard
NASA Langley Research Center
Hampton, VA 23681-2199

## 2.1 Title of Investigation

Clouds and the Earth's Radiant Energy System (CERES)
ERBE-like Subsystems (Subsystems 2.0 & 3.0)

## 2.2 Contact Information

Dr. Kory J. Priestley, Subsystem 2.0 Working Group Chair
E-mail: K.J.Priestley@LaRC.NASA.Gov
Telephone: (757) 864-8147

Dr. Takmeng Wong, Subsystem 2.0 Working Group Science and Validation Advisor
E-mail: Takmeng.Wong@LaRC.NASA.Gov
Telephone: (757) 864-5607

FAX: (757) 864-7996
Mail Stop 420
Atmospheric Sciences Competency
Building 1250
21 Langley Boulevard
NASA Langley Research Center
Hampton, VA 23681-2199

Edward A. Kizer, Subsystem 2.0 Software and Data Management Lead
E-mail: E.A.Kizer@LaRC.NASA.Gov
Telephone: (757) 827-4883
FAX: (757) 864-7996
Science Applications International Corporation (SAIC)
One Enterprise Parkway, Suite 300
Hampton, VA 23666-5845

## 3.0 Origination

The CERES data originate from CERES instruments on-board either the TRMM, Terra or Aqua EOS Earth-orbiting spacecrafts. Table 3-1 lists the CERES instruments and their host satellites.

Table 3-1. CERES Instruments

| Satellite | CERES Instrument | |
|---|---|---|
| TRMM | PFM | |
| Terra | FM1 | FM2 |
| Aqua | FM3 | FM4 |

The CERES instrument contains three scanning thermistor bolometer radiometers that measure the radiation in the near-visible through far-infrared spectral region. The shortwave detector measures Earth-reflected and Earth-emitted solar radiation and the window detector measures Earth-emitted longwave radiation in the water vapor window. The total detector measures total Earth-reflected and Earth-emitted radiation. The detectors are coaligned and mounted on a spindle that rotates about the instrument elevation axis. The resolution of the CERES radiometers is usually referenced to the optical FOV (See Note-3.3).

The CERES instrument has an operational scanning cycle of 6.6 seconds and various scan elevation profiles. Radiometric measurements are sampled from the detectors every 0.01 seconds in all scanning profiles. The instrument makes Earth-viewing science measurements while the detectors rotate in the vertical (elevation scan) plane, and while the instrument horizontal (azimuth scan) plane is either fixed or rotating. The instrument has built-in calibration sources for performing in-flight calibrations, and can also be calibrated by measuring solar radiances reflected by a solar diffuser plate into the instrument field of view. See the In-flight Measurement Analysis document, DRL 64, provided by the CERES instrument builder TRW (Reference 3), and the CERES ATBD for Subsystem 1.0 (Reference 4).

# 4.0 Data Description

## 4.1 Spatial Characteristics

### 4.1.1 Spatial Coverage

The CERES collection is a global data set whose spatial coverage depends on the satellite orbit. The spatial coverage of the data contained on the ES-8 is shown in Table 4-1.

Table 4-1. ES-8 Spatial Coverage

| Spacecraft | Instrument | Minimum Latitude (deg) | Maximum Latitude (deg) | Minimum Longitude (deg) | Maximum Longitude (deg) | Spacecraft Altitude (km) |
|---|---|---|---|---|---|---|
| TRMM | PFM | -45 | 45 | -180 | 180 | 350 |
| Terra | FM1 & FM2 | -90 | 90 | -180 | 180 | 705 |
| Aqua | FM3 & FM4 | -90 | 90 | -180 | 180 | 705 |

### 4.1.2 Spatial Resolution

The ES-8 contains measurement level data as described in this document's Summary. The CERES FOV for a nadir viewing measurement is 10 km for TRMM and 20 km for both Terra and Aqua.

## 4.2 Temporal Characteristics

### 4.2.1 Temporal Coverage

CERES temporal coverage begins at different times depending upon when the spacecraft is launched, when the scan covers are opened after launch, and when early in-orbit calibration check-out is completed (See Table 4-2). The ES-8 contains 24 hours of data beginning at midnight GMT.

Table 4-2. CERES Temporal Coverage

| Spacecraft | Instrument | Launch Date | Start Date | End Date |
|---|---|---|---|---|
| TRMM | PFM | 11/27/1997 | 12/27/1997 | 8/31/1998[a] |
| Terra | FM1 & FM2 | 12/18/1999 | 02/24/2000 | TBD |
| Aqua | FM3 & FM4 | 05/05/2002 | 06/19/2002 | TBD |

a. The CERES instrument on TRMM has operated only occasionally since 9/1/98 due to a power converter anomaly.

### 4.2.2 Temporal Resolution

The ES-8 contains measurement level data as explained in this document's Summary. These measurements are organized on the ES-8 according to 3.3-second scans in 6.6-second records. Each record contains 660 measurements. The measurement frequency is one per 0.01 seconds. Table 4-3 shows the orbit inclination, altitude, and approximate number of Earth viewing measurements per record for each CERES spacecraft.

Table 4-3. CERES Orbit Characteristics

| Spacecraft | Inclination | Altitude | Number of Earth-viewing Measurements |
|---|---|---|---|
| TRMM | 35° | 350 km | 500 |
| Terra | Sun-synchronous 10:30 a.m. Polar | 705 km | 390 |
| Aqua | Sun-synchronous 1:30 p.m. Polar | 705 km | 390 |

## 4.3 Parameter Definitions

The ES-8 data product has been documented with several different elements. Acronyms and Units are explained in Section 16.0. Some acronyms are linked to glossary "Terms" in Section 15.0 which expand the description to a paragraph length. The formal definitions of the ES-8 parameters are in Section 4.3 and begin with a short statement of the parameter followed by the units, range, and a link to a table which gives data type and dimension information. Following the short definition is a more complete definition, which may include additional information of less interest to some. When necessary, "Notes" in Section 8.0 are given to expand on subjects that will help in the use and understanding of the ES-8 product. Notes are generally characterized by more details and longer length.

### 4.3.1 ES-8 Vdata

#### ES8-V1 Time at observation

The Julian Date (See Term-10) at scan sample 1 (See Term-18). (day) [2440000 .. 2480000] (See Table 5-4)

The time of observation for any scan sample (See Term-18) is

$$t_n = t_1 + (n-1)\left(\frac{0.01\ \text{sec}}{24 \times 60 \times 60\ \text{sec day}^{-1}}\right)$$

where $t_1$=(ES8-V1) and n=scan sample number from 1 to 660.

In Subsystem 1, the toolkit call PGS_TD_SCtime_to_UTC converts Spacecraft time to UTC time. A second toolkit call, PGS_TD_UTCtoUTCjd, converts the ASCII string into two double precision real numbers, the Julian Date at Greenwich midnight and the fraction of the day since Greenwich midnight, which are added together to obtain the time of observation.

### ES8-V2 Earth-Sun distance at record start

The distance from the Earth to the Sun in AU at the scan sample 1 (See Term-18). (AU) [0.98 .. 1.02] (See Table 5-4)

In Subsystem 1, the toolkit call PGS_CBP_CB_Vector computes the Earth-Centered Inertial frame vector to the Sun. The toolkit call PGS_CSC_ECItoECR transforms the position vector to the ECR or Earth equator, Greenwich meridian system (See Term-3). The magnitude of the position vector is then computed and converted from meters to AU.

### ES8-V3 X component of satellite position at record start

The X component of the satellite position at scan sample 1 (See Term-18) in the Earth equator, Greenwich meridian system (See Term-3). (m) [$-8\times10^6$ .. $8\times10^6$] (See Table 5-4)

In Subsystem 1, the toolkit call PGS_EPH_Earth_EphemAttit computes the satellite position and velocity vector in Earth-Centered Inertial coordinates. A second toolkit call, PGS_CSC_ECItoECR, transforms the position and velocity vector to the ECR or Earth equator, Greenwich meridian system (See Term-3).

### ES8-V4 X component of satellite position at record end

The X component of the satellite position at scan sample 660 (See Term-18) in the Earth equator, Greenwich meridian system (See Term-3). (m) [$-8\times10^6$ .. $8\times10^6$] (See Table 5-4)

The satellite position components are determined from toolkit calls (See ES8-V3).

### ES8-V5 Y component of satellite position at record start

The Y component of the satellite position at scan sample 1 (See Term-18) in the Earth equator, Greenwich meridian system (See Term-3). (m) [$-8\times10^6$ .. $8\times10^6$] (See Table 5-4)

The satellite position components are determined from toolkit calls (See ES8-V3).

### ES8-V6 Y component of satellite position at record end

The Y component of the satellite position at scan sample 660 (See Term-18) in the Earth equator, Greenwich meridian system (See Term-3). (m) [$-8\times10^6$ .. $8\times10^6$] (See Table 5-4)

The satellite position components are determined from toolkit calls (See ES8-V3).

### ES8-V7 Z component of satellite position at record start

The Z component of the satellite position at scan sample 1 (See Term-18) in the Earth equator, Greenwich meridian system (See Term-3). (m) [$-8\times10^6$ .. $8\times10^6$] (See Table 5-4)

The satellite position components are determined from toolkit calls (See ES8-V3).

### ES8-V8 Z component of satellite position at record end

The Z component of the satellite position at scan sample 660 (See Term-18) in the Earth equator, Greenwich meridian system (See Term-3). (m) [$-8\times10^6$ .. $8\times10^6$] (See Table 5-4)

The satellite position components are determined from toolkit calls (See ES8-V3).

### ES8-V9 X component of satellite velocity at record start

The X component of the satellite inertial velocity at scan sample 1 (See Term-18) in the Earth equator, Greenwich meridian system (See Term-3). (m $sec^{-1}$) [$-1\times10^4$ .. $1\times10^4$] (See Table 5-4)

The satellite velocity components are determined from toolkit calls (See ES8-V3).

### ES8-V10 X component of satellite velocity at record end

The X component of the satellite inertial velocity at scan sample 660 (See Term-18) in the Earth equator, Greenwich meridian system (See Term-3). (m $sec^{-1}$) [$-1\times10^4$ .. $1\times10^4$] (See Table 5-4)

The satellite velocity components are determined from toolkit calls (See ES8-V3).

### ES8-V11 Y component of satellite velocity at record start

The Y component of the satellite inertial velocity at scan sample 1 (See Term-18) in the Earth equator, Greenwich meridian system (See Term-3). (m $sec^{-1}$) [$-1\times10^4$ .. $1\times10^4$] (See Table 5-4)

The satellite velocity components are determined from toolkit calls (See ES8-V3).

### ES8-V12 Y component of satellite velocity at record end

The Y component of the satellite inertial velocity at scan sample 660 (See Term-18) in the Earth equator, Greenwich meridian system (See Term-3). (m $sec^{-1}$) [$-1\times10^4$ .. $1\times10^4$] (See Table 5-4)

The satellite velocity components are determined from toolkit calls (See ES8-V3).

### ES8-V13 Z component of satellite velocity at record start

The Z component of the satellite inertial velocity at scan sample 1 (See Term-18) in the Earth equator, Greenwich meridian system (See Term-3). (m $sec^{-1}$) [$-1\times10^4$ .. $1\times10^4$] (See Table 5-4)

The satellite velocity components are determined from toolkit calls (See ES8-V3).

### ES8-V14 Z component of satellite velocity at record end

The Z component of the satellite inertial velocity at scan sample 660 (See Term-18) in the Earth equator, Greenwich meridian system (See Term-3). (m $sec^{-1}$) [$-1\times10^4$ .. $1\times10^4$] (See Table 5-4)

The satellite velocity components are determined from toolkit calls (See ES8-V3).

### ES8-V15 Colatitude of satellite nadir at record start

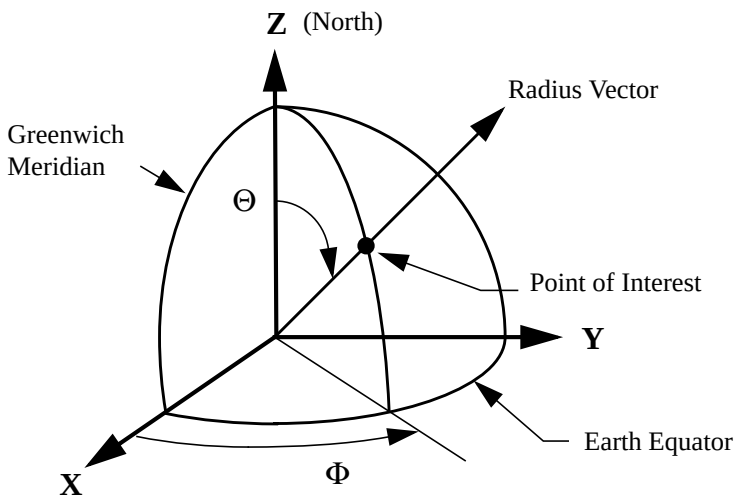


Figure 4-1. Colatitude and Longitude

The geocentric colatitude angle Θ (See Figure 4-1) of the satellite nadir point (See Term-11) at scan sample 1 (See Term-18) in the Earth equator, Greenwich meridian system (See Term-3). (deg) [0 .. 180] (See Table 5-4)

The geocentric colatitude of nadir is the angle between the vector from the center of the Earth to the satellite and a vector normal to the Earth equator toward the North pole as defined in the Earth equator, Greenwich meridian system (See Term-3). An alternate formulation is given in Note-2.

In Subsystem 1, the toolkit call PGS_EPH_EphemAttit computes the satellite position vector in Earth-Centered Inertial coordinates. A second toolkit call, PGS_CSC_ECItoECR, transforms the position vector to the ECR or Earth equator, Greenwich meridian rectangular coordinate system and from this, the geocentric colatitude and longitude are calculated.

### ES8-V16 Colatitude of satellite nadir at record end

The geocentric colatitude angle Θ (See Figure 4-1) of the satellite nadir point (See Term-11) at scan sample 660 (See Term-18) in the Earth equator, Greenwich meridian system (See Term-3). (deg) [0 .. 180] (See Table 5-4)

The geocentric colatitude of nadir is the angle between the vector from the center of the Earth to the satellite and a vector normal to the Earth equator toward the North pole as defined in the Earth equator, Greenwich meridian system (See Term-3). An alternate formulation is given in Note-2.

### ES8-V17 Longitude of satellite nadir at record start

The longitude angle Φ (See Figure 4-1) of the satellite nadir point (See Term-11) at scan sample 1 (See Term-18) in the Earth equator, Greenwich meridian system (See Term-3). (deg) [0 .. 360] (See Table 5-4)

The longitude of nadir is the angle in the Earth equator plane from the Greenwich meridian (See Term-3) to the nadir point meridian, rotating East. An alternate formulation is given in Note-2.

### ES8-V18 Longitude of satellite nadir at record end

The longitude angle Φ (See Figure 4-1) of the satellite nadir point (See Term-11) at scan sample 660 (See Term-18) in the Earth equator, Greenwich meridian system (See Term-3). (deg) [0 .. 360] (See Table 5-4)

The longitude of nadir is the angle in the Earth equator plane from the Greenwich meridian (See Term-3) to the nadir point meridian, rotating East. An alternate formulation is given in Note-2.

### ES8-V19 Colatitude of Sun at observation

The geocentric colatitude angle of the Sun at scan sample 1 (See Term-18) in the Earth equator, Greenwich meridian system (See Term-3). (deg) [0 .. 180] (See Table 5-4)

The geocentric colatitude of the Sun is the angle between the vector from the center of the Earth to the Sun and a vector normal to the Earth equator toward the North pole as defined in the Earth equator, Greenwich meridian system (See Term-3).

In Subsystem 1, the toolkit call PGS_CBP_Earth_CB_vector computes the sun position vector in Earth-Centered Inertial coordinates. A second toolkit call, PGS_CSC_ECItoECR, transforms the position vector to the ECR or Earth equator, Greenwich meridian rectangular coordinate system and from this, the geocentric colatitude and longitude are calculated.

### ES8-V20 Longitude of Sun at observation

The longitude angle of the Sun at scan sample 1 (See Term-18) in the Earth equator, Greenwich meridian system (See Term-3). (deg) [0 .. 360] (See Table 5-4)

The longitude of the Sun is the angle in the Earth equator plane from the Greenwich meridian (See Term-3) to the Sun meridian, rotating East.

### ES8-V21 Spectral Response Functions

The spectral response functions are spectral response values (unitless) [0 .. 1] at given wavelengths (microns) for the shortwave, total, and window channels used to create the spectral correction coefficients (See Term-20).

Spectral response function represent the spectral throughput of the detector optical component elements. The spectral response functions are used to spectrally correct the measured radiances that are passed through the optical path of each individual detector to obtain the unfiltered radiances dependent on the scene type (See ES8-14).

## 4.3.2 ES-8 Scientific Data Definitions

### ES8-1 Colatitude of CERES FOV at TOA

This parameter is the geocentric colatitude angle Θ (See Figure 4-1) of the TOA point (See Term-23). (deg) [0 .. 180] (See Table 5-3)

The geocentric colatitude of the TOA point is the angle between the vector from the center of the Earth to the TOA point (See Term-23) and a vector normal to the Earth equator toward the North pole as defined in the Earth equator, Greenwich meridian system (See Term-3).

If any part of the FOV is off the Earth "surface" (See Term-4), the FOV flag (See ES8-18) is set to bad and the colatitude is set to default. There are 660 values of this parameter per record; one for each measurement point (See Term-17).

In Subsystem 1, the toolkit call PGS_CSC_GetFOV_Pixel returns the geodetic latitude and longitude of the intersection of the FOV centroid and the CERES_TOA model. Another toolkit call PGS_CSC_GEOtoECR transforms the geodetic latitude and longitude to the ECR or Earth equator, Greenwich meridian rectangular coordinates from which the geocentric colatitude and longitude are calculated.

### ES8-2 Longitude of CERES FOV at TOA

This parameter is the longitude angle Φ (See Figure 4-1) of the TOA point (See Term-23). (deg) [0 .. 360] (See Table 5-3)

The longitude of the TOA point is the angle in the Earth equator plane from the Greenwich meridian (See Term-3) to the TOA point meridian, rotating East.

If any part of the FOV is off the Earth "surface" (See Term-4), the FOV flag (See ES8-18) is set to bad and the longitude is set to default. There are 660 values of this parameter per record; one for each measurement (See Term-17).

The longitude of the TOA point is determined from toolkit calls (See ES8-1).

### ES8-3 CERES TOT filtered radiance

This parameter is the measured, spectrally integrated radiance emerging from the TOA, where the spectral integration is weighted by the spectral throughput of the TOT channel. It is the "raw" measurement from the TOT channel after count conversion (See Term-2) and is spectrally corrected (See Term-20) to yield the unfiltered LW radiance (See ES8-10) at night. The TOT and SW filtered radiances are spectrally corrected together to yield the LW radiance during the day. ($W\ m^{-2}\ sr^{-1}$) [-2 .. 700] (See Table 5-3)

The value of the filtered TOT radiance is defined as either "good" or "bad" by the quality flag (See ES8-15). If the value is "bad," for any reason, the TOT filtered radiance is set to a default value (See Section 4.4). If the value is "good," the measured value is retained. There are 660 values of TOT filtered radiance per record; one for each measurement point (See Term-17).

The TOT filtered radiance is a measure of all radiance that passes through the TOT channel. The spectral weighting produced by the TOT channel throughput is the product of the primary mirror reflectance, the secondary mirror reflectance, and the absorptance of the detector flake. The TOT spectral throughput passes about 90% of the radiant power with wavelengths longer than 5 μm and about 85% of the power with shorter wavelengths.

### ES8-4 CERES SW filtered radiance

This parameter is the measured, spectrally integrated radiance emerging from the TOA, where the spectral integration is weighted by the spectral throughput of the SW channel. It is the "raw" measurement from the SW channel after count conversion (See Term-2) and is spectrally corrected (See Term-20) to yield the unfiltered SW radiance (See ES8-9). ($W\ m^{-2}\ sr^{-1}$) [-4 .. 510] (See Table 5-3)

The value of the SW filtered radiance is defined as either "good" or "bad" by the quality flag (See ES8-16). If the value is "bad," for any reason, the SW filtered radiance is set to a default value (See Section 4.4). If the value is "good" the measured value is retained. There are 660 values of SW filtered radiance per record; one for each measurement point (See Term-17).

The SW filtered radiance is a measure of all radiance that passes through the SW channel. The spectral weighting produced by the SW channel throughput is the product of the SW filter throughput and the TOT channel throughput (See ES8-3). The SW spectral throughput passes about 75% of the radiant power with wavelengths shorter than 5 µm and cuts off rather sharply at about 5 µm. Wavelengths longer than this wavelength contribute a very small fraction of this measurement.

### ES8-5 CERES WN filtered radiance

This parameter is a measured, spectrally integrated radiance emerging from the TOA, where the spectral integration is weighted by the spectral throughput of the WN channel. It has a bandpass from approximately 8 to 12 µm. It is the "raw" measurement from the window channel after count conversion (See Term-2) and is spectrally corrected (See Term-20) to yield the unfiltered WN radiance (See ES8-11). ($W\ m^{-2}\ sr^{-1}\mu m^{-1}$) [-1 .. 15] (See Table 5-3)

The value of the WN filtered radiance is defined as either "good" or "bad" by the quality flag (See ES8-17). If the value is "bad," for any reason, the WN filtered radiance is set to a default value (See Section 4.4). If the value is "good," the measured value is retained. There are 660 values of WN filtered radiance per record; one for each measurement point (See Term-17).

The WN filtered radiance is a measure of all radiance that passes through the WN channel. The spectral weighting produced by the WN channel throughput is the product of the WN filter throughput and the TOT channel throughput (See ES8-3). The WN spectral throughput passes about 67% of the radiant power between 8 to 12 µm.

### ES8-6 CERES viewing zenith at TOA

This parameter is the zenith angle θ (See Figure 4-2) at the TOA point (See Term-23) of the satellite. (deg) [0 .. 90] (See Table 5-3)

The viewing zenith is the angle between the radius vector from the center of the Earth to the TOA point and a vector from the TOA point to the satellite. There are 660 values of viewing zenith per record; one for each measurement point (See Term-17).

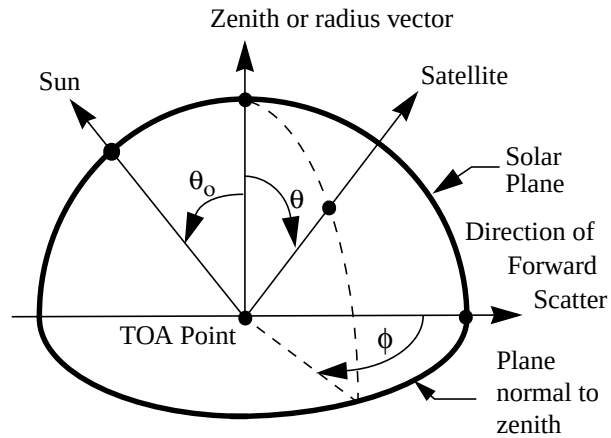


Figure 4-2. Viewing Angles at TOA

### ES8-7 CERES solar zenith at TOA

This parameter is the zenith angle $\theta_o$ (See Figure 4-2) at the TOA point (See Term-23) of the Sun. (deg) [0 .. 180] (See Table 5-3)

The solar zenith is the angle between the radius vector from the center of the Earth to the TOA point and a vector from the TOA point to the Sun. There are 660 values of solar zenith per record; one for each measurement point (See Term-17).

### ES8-8 CERES relative azimuth at TOA

This parameter is the azimuth angle ϕ (See Figure 4-2) at the TOA point (See Term-23) of the satellite relative to the solar plane. (deg) [0 .. 360] (See Table 5-3)

The relative azimuth is measured clockwise in the plane normal to the zenith so that the relative azimuth of the Sun is always $180^o$. The solar plane is the plane which contains the radius vector (zenith) and a vector from the TOA point to the Sun. If the TOA point is north of the subsolar point (See Term-21) on the same meridian, then an azimuth of $90^o$ would imply the satellite is east of the TOA point. There are 660 values of relative azimuth per record; one for each measurement point (See Term-17).

### ES8-9 CERES SW unfiltered radiance

This parameter is an estimate of the solar radiance at all wavelengths reflected back into space and contains no thermal radiance. ($W\ m^{-2}\ sr^{-1}$) [-10 .. 510] (See Table 5-3)

It is a spectrally integrated radiance that is intended to represent the radiance of reflected sunlight. In other words, the SW unfiltered radiance is the radiance we would observe if we had a spectrally flat channel that passed all the reflected sunlight and that removed any thermal emission from the Earth and the Earth's atmosphere. Frequently, in informal discussion, we incorrectly refer to the SW unfiltered radiance as a broadband radiance covering the spectral interval from 0 to 5 μm.

At night the SW radiance is set to zero where night is defined as a solar zenith angle (ES8-7) greater than $90^o$ at the TOA point (See Term-23). During the day, the SW radiance, $I^{SW}$, is

defined by $I^{SW} = C^{SW} (m_f^{SW} - \mathrm{SW}^{offset})$ where $C^{SW}$ is from a set of spectral correction coefficients (See Term-20), $m_f^{SW}$ is the filtered shortwave measurement (ES8-4), and $\mathrm{SW}^{offset}$ is an estimate of the thermal radiance measured by the shortwave channel and is either zero or the average nighttime shortwave measurement for the previous nighttime passage. $\mathrm{SW}^{offset}$ is updated each satellite revolution or as often as 15 times for a 24-hour period.

There are 660 values of the SW unfiltered radiance per record; one for each measurement point (See Term-17).

The unfiltered SW radiance is "good" if it contains a non-default value. If the filtered SW radiance is flagged "bad" (See ES8-16), then the unfiltered SW radiance is set to default (See Section 4.4). If the FOV Flag is "bad" (See ES8-18), or the SW ADM is greater than 2 (See Note-4), then the unfiltered SW radiance is set to default. No other condition will cause the SW unfiltered radiance on the ES-8 to be set to default.

### ES8-10 CERES LW unfiltered radiance

This parameter is an estimate of the thermal radiance at all wavelengths emitted to space including shortwave thermal radiance and including no solar reflected radiance. ($W\ m^{-2}\ sr^{-1}$) [0 .. 200] (See Table 5-3)

It is a spectrally integrated radiance that is intended to represent the radiance from emission of the atmosphere and the Earth that emerges from the top of the atmosphere. In other words, the LW unfiltered radiance is the radiance that we would observe if we had a spectrally flat channel that passed all the emitted radiance and that removed any reflected sunlight. Frequently, in informal discussion, we incorrectly refer to the LW unfiltered radiance as a broadband radiance covering wavelengths longer than 5 µm.

At night the LW radiance $I^{LW}$ is defined by $I^{LW} = C^{TOT}\ m_f^{TOT}$ where $C^{TOT}$ is from a set of spectral correction coefficients (See Term-20), $m_f^{TOT}$ is the filtered total measurement (See ES8-3, and where night is defined as a solar zenith angle (See ES8-7) greater than $90^o$ at the TOA point (See Term-23). During the day, the LW radiance is defined as the TOT radiance minus the SW radiance with the appropriate spectral correction coefficients, or by $I^{LW} = C^{TOT}\ m_f^{TOT} + C^{SW} (m_f^{SW} - \mathrm{SW}^{offset})$ where $C^{TOT}$ and $C^{SW}$ are from a set of spectral correction coefficients (See Term-20), $m_f^{SW}$ is the filtered shortwave measurement (See ES8-4), and $\mathrm{SW}^{offset}$ is an estimate of the thermal radiation in the shortwave measurement (See ES8-9).

There are 660 values of the LW unfiltered radiance per record; one for each measurement point (See Term-17).

The unfiltered LW radiance is "good" if it contains a non-default value. If the filtered TOT radiance is flagged "bad " (See ES8-15), then the unfiltered LW radiance is set to default (See Section 4.4). During the day, the unfiltered LW radiance is set to default if the filtered SW radiance is

flagged "bad." If the FOV Flag is "bad" (See ES8-18), or the SW ADM is greater than 2 (See Note-4), then the unfiltered LW radiance is set to default. No other condition will cause the LW unfiltered radiance on the ES-8 to be set to default.

The spectral correction (See Term-20) which converts the filtered radiance to unfiltered radiance is dependent on the scene type (See ES8-14). If the SW ADM is greater than 2, then the scene identified by the MLE (See Note-5) is questionable and the spectral correction is not performed. This will result in default values for both the unfiltered radiance and flux (See ES8-13).

### ES8-11 CERES WN unfiltered radiance

This parameter is an estimate of the average radiance per micrometer in the spectral window from 8.0 to 12.0 microns. This radiance is dominated by emission from the Earth's surface when the scene is clear. ($W\ m^{-2}\ sr^{-1} \mu m^{-1}$) [0 .. 15] (See Table 5-3)

The unfiltered WN radiance is defined by $I^{WN} = C^{WN}\ m_f^{WN}$ where $C^{WN}$ is from a set of spectral correction coefficients (See Term-20), and $m_f^{WN}$ is the filtered window measurement (See ES8-5). There are 660 values of the WN unfiltered radiance per record; one for each measurement point (See Term-17).

The unfiltered WN radiance is "good" if it contains a non-default value. If the filtered WN radiance is flagged "bad" (See ES8-17), then the unfiltered WN radiance is set to default (See Section 4.4). If the FOV Flag is "bad" (See ES8-18), or the SW ADM is greater than 2 (See Note-4), then the unfiltered WN radiance is set to default. No other condition will cause the WN unfiltered radiance on the ES-8 to be set to default.

The spectral correction (See Term-20) which converts the filtered radiance to unfiltered radiance is dependent on the scene type (See ES8-14). If the SW ADM is greater than 2, then the scene identified by the MLE (See Note-5) is questionable and the spectral correction is not performed. This will result in a default value for the WN unfiltered radiance.

### ES8-12 CERES SW flux at TOA

This parameter is an estimate of the solar flux at all wavelengths reflected back into space at the TOA point (See Term-23). ($W\ m^{-2}$) [0 .. 1400] (See Table 5-3)

At night the SW flux is set to zero where night is defined as a solar zenith angle (See ES8-7) greater than $90^o$ at the TOA point (See Term-23). The SW flux is set to default (See Section 4.4) when the solar zenith angle is between $86.5^o$ and $90.0^o$. When the solar zenith is less than or equal to $86.5^o$, the SW flux $\hat{M}^{SW}$ is given by

$$\hat{M}^{SW} = \frac{\pi\ I^{SW}}{R^{i}(\theta, \phi, \theta_o)}$$

where $I^{SW}$ is the shortwave radiance (See ES8-9), and R is the anisotropy (or ADM, See Note-4) for the i$^{th}$ scene type (See ES8-14); and R is evaluated at the viewing zenith angle $\theta$ (See ES8-6), relative azimuth angle $\phi$ (See ES8-8), and solar zenith angle $\theta_o$ (See ES8-7).

There are 660 values of the SW flux per record; one for each measurement point (See Term-17).

The SW flux is set to default if the SW radiance (See ES8-9) is default, or if the scene type (See ES8-14) is unknown, or if the instrument is operating in the rapid retrace mode (ES8-19). During the day, $albedo = \hat{M}^{SW}/(E\cos\theta_o)$ where E=1365 d$^{-2}$ and d=(ES8-V2). If albedo is greater than 1.0 or less than 0.02, the SW flux is set to default. The SW flux is also set to default for geometric conditions that lead to inaccurate flux estimates, or for $\theta > 70^o$, $86.5^o < \theta_o \le 90^o$, and $R^i \ge 2$.

### ES8-13 CERES LW flux at TOA

This parameter is an estimate of the thermal flux at all wavelengths emitted to space at the TOA point (See Term-23) including shortwave thermal flux. (W m$^{-2}$) [50 .. 450] (See Table 5-3)

The LW flux $\hat{M}^{LW}$ is given by

$$\hat{M}^{LW} = \frac{\pi I^{LW}}{R^i(\theta, \Theta)}$$

where $I^{LW}$ is the longwave radiance (See ES8-10), and R is the anisotropy (or ADM, See Note-4) for the i$^{th}$ scene type (See ES8-14); and R is evaluated at the viewing zenith angle $\theta$ (See ES8-6), and colatitude of the TOA point $\Theta$ (See ES8-1).

There are 660 values of the LW flux per record; one for each measurement point (See Term-17).

The LW flux is set to default (See Section 4.4) if the LW radiance (See ES8-10) is default, or if the scene type (See ES8-14) is unknown, or if the instrument is operating in the rapid retrace mode (See ES8-19), or if the flux is greater than 400 W m$^{-2}$ or less than 50 W m$^{-2}$. The LW flux is also set to default for geometric conditions that lead to inaccurate flux estimates, or for $\theta > 70^o$.

### ES8-14 ERBE scene identification at observation

This parameter is an estimate of the scene at the TOA point as determined by the MLE scene identification algorithm (See Note-5). (N/A) [0 .. 12.4] (See Table 5-3)

The 13 possible ERBE scene types are listed in Table 4-4.

Table 4-4. ERBE Scene Types

| ES8-14 VALUE | DESCRIPTION OF SCENE | Cloud Cover |
|---|---|---|
| 0.X | unknown scene | |
| 1.X | clear ocean | 0 - 5 % |
| 2.X | clear land | 0 - 5 % |
| 3.X | clear snow | 0 - 5 % |
| 4.X | clear desert | 0 - 5 % |
| 5.X | clear land-ocean mix | 0 - 5 % |
| 6.X | partly cloudy over ocean | 5 - 50 % |
| 7.X | partly cloudy over land or desert | 5 - 50 % |
| 8.X | partly cloudy over land-ocean mix | 5 - 50 % |
| 9.X | mostly cloudy over ocean | 50 - 95 % |
| 10.X | mostly cloudy over land or desert | 50 - 95 % |
| 11.X | mostly cloudy over land-ocean mix | 50 - 95 % |
| 12.X | overcast | 95 - 100 % |

where a land-ocean mix scene denotes 50% land and 50% ocean and is used for coastal areas and where X equals 0, 1, 2, 3, 4 for ocean, land, snow, desert, land-ocean mix, respectively. The decimal defines the geographic scene so that 12.1 would indicate overcast over land, etc. Care should be taken in determining the geographic scene from the decimal because of computer characteristics. A useful Fortran code is

```
ISCENE = NINT(ES8-14)

IX = NINT(((ES8-14) - REAL(ISCENE)) * 10.0)
```

where NINT is the nearest integer operator and IX is the geographic scene index.

There are 660 values of the ERBE scene per record; one for each measurement point (See Term-17).

### ES8-15 TOT channel flag words

This parameter contains twenty two 32-bit words where a single bit defines the quality of the filtered TOT radiance (See ES8-3) as “good” (bit=0) or “bad” (bit=1). There are 660 bit flags per record; one for each measurement point (See Term-17). (N/A) [N/A] (See Table 5-3)

The ordering of the bit flags is given in Table 4-5 where bit 32 is the “sign” bit and bit 31 is extra so that we have 22 words × 30 bits = 660 bit flags.

Table 4-5. Bit Order for Radiometric and FOV Quality Flags

| | Bit Order | | | | | | | | |
|---|---|---|---|---|---|---|---|---|---|
| **Word** | **32[a]** | **31[b]** | **30** | **29** | **28** | **27 ... 4** | **3** | **2** | **1** |
| 1 | | | 30 | 29 | 28 | | 3 | 2 | 1 |
| 2 | | | 60 | 59 | 58 | | 33 | 32 | 31 |
| 3 | | | 90 | 89 | 88 | | 63 | 62 | 61 |
| ... | | | | | | | | | |
| 20 | | | 600 | 599 | 598 | | 573 | 572 | 571 |
| 21 | | | 630 | 629 | 628 | | 603 | 602 | 601 |
| 22 | | | 660 | 659 | 658 | | 633 | 632 | 631 |

a. Sign Bit
b. Extra Bit

### ES8-16 SW channel flag words

This parameter contains twenty two 32-bit words where a single bit defines the quality of the filtered SW radiance (See ES8-4) as “good” (bit=0) or “bad” (bit=1). There are 660 bit flags per record; one for each measurement point (See Term-17). (N/A) [N/A] (See Table 5-3)

The ordering of the bit flags is given in Table 4-5 where bit 32 is the “sign” bit and bit 31 is extra so that we have 22 words × 30 bits = 660 bit flags.

### ES8-17 WN channel flag words

This parameter contains twenty two 32-bit words where a single bit defines the quality of the filtered WN radiance (See ES8-5) as “good” (bit=0) or “bad” (bit=1). There are 660 bit flags per record; one for each measurement point (See Term-17). (N/A) [N/A] (See Table 5-3)

The ordering of the bit flags is given in Table 4-5 where bit 32 is the “sign” bit and bit 31 is extra so that we have 22 words × 30 bits = 660 bit flags.

### ES8-18 Scanner FOV flag words

This parameter contains twenty two 32-bit words where a single bit defines the quality of the FOV as “good” (bit=0) or “bad” (bit=1). A good FOV falls entirely on the surface (not TOA) of the Earth (See Term-6). All other FOVs are flagged bad. There are 660 bit flags per record; one for each measurement point (See Term-17). (N/A) [N/A] (See Table 5-3)

The ordering of the bit flags is given in Table 4-5 where bit 32 is the “sign” bit and bit 31 is extra so that we have 22 words × 30 bits = 660 bit flags.

### ES8-19 Rapid retrace flag words

This parameter contains twenty two 32-bit words where a single bit defines the state of the scan rate as “not in rapid retrace” (bit=0) or “in rapid retrace” (bit=1). Rapid retrace (See Term-13) occurs during the short scan mode (See ES8-20). There are 660 rapid retrace bit flags per record; one for each measurement point (See Term-17). (N/A) [N/A] (See Table 5-3)

The ordering of the bit flags is given in Table 4-5 where bit 32 is the “sign” bit and bit 31 is extra so that we have 22 words × 30 bits = 660 bit flags.

### ES8-20 Scanner operations flag word

This parameter contains three 32-bit words which define the scanner operations during the 6.6-sec record. The individual bits are defined in Table 4-6, Table 4-7, and Table 4-8. Additional details follow the tables. (N/A) [N/A] (See Table 5-3)

Table 4-6. Scanner Operations Flag Word 1 (of 3)

| Bit Position (Right to Left) | Bit Value | Detail Description | Meaning |
|---|---|---|---|
| 0-3 | | ES8-20-A | The Instrument is in the following Mode: |
| | 0000 | | Safe Mode |
| | 0001 | | Standby Mode |
| | 0010 | | Crosstrack Mode |
| | 0011 | | Biaxial Mode |
| | 0100 | | Solar Calibration Mode |
| | 0101 | | Diagnostic Configuration Mode |
| | 0110 | | Internal Calibration Mode |
| | 0111 | | Special Short Scan Mode |
| | 1000 | | Contamination Safe Mode |
| | 1001 | | Hold Mode |
| | 1010 | | Abbreviated Internal Calibration Mode |
| | 1011 | | Fixed Azimuth Mode |
| | 1100-1111 | | Undefined |
| 4-5 | 00 | | Elevation Motor Drive Enabled |
| | 01 | | Elevation Motor Drive Disabled |
| | 10,11 | | Undefined |
| 6-7 | 00 | | Azimuth Motor Drive Enabled |
| | 01 | | Azimuth Motor Drive Disabled |
| | 10,11 | | Undefined |
| 8-9 | 00 | | Instrument Previous Mode (See bit 0-3) not in Solar Calibration or Internal Calibration |
| | 01 | | Instrument Previous Mode in Solar Calibration |
| | 10 | | Instrument Previous Mode in Internal Calibration |
| | 11 | | Undefined |
| 10-11 | 00 | | Instrument not in Internal Calibration |
| | 01 | | Instrument in Internal Calibration |
| | 10,11 | | Undefined |

Table 4-6. Scanner Operations Flag Word 1 (of 3)

| Bit Position (Right to Left) | Bit Value | Detail Description | Meaning |
|---|---|---|---|
| 12-14 | 000<br>001<br>010<br>011<br>100-111 | | SWICS Lamp off<br>SWICS Intensity at Level 1<br>SWICS Intensity at Level 2<br>SWICS Intensity at Level 3<br>Undefined |
| 15-30 | | | Spares |
| 31 | 0<br><br><br><br>1 | | At least one scanner radiometric value (ES8-3 - ES8-5) has both a good radiometric flag (ES8-15 - ES8-17) and a good FOV flag (ES8-18)<br>If the above situation does not exist, record will not be included on the ES-8 product. |

See detail descriptions after Table 4-8.

Table 4-7. Scanner Operations Flag Word 2 (of 3)

| Bit Position (Right to Left) | Bit Value | Detail Description | Meaning |
|---|---|---|---|
| 0-4 | | ES8-20-B | The Scanner is in the following Elevation Scan Profiles: |
| | 00000 | | Stow |
| | 00001 | | Normal Earth Scan |
| | 00010 | | Short Earth Scan |
| | 00011 | | MAM Scan |
| | 00100 | | Nadir Scan |
| | 00101 | | Scan Profile 6 |
| | 00110 | | Scan Profile 7 |
| | 00111 | | Scan Profile 8 |
| | 01000 | | Scan Profile 9 |
| | 01001 | | Scan Profile 10 |
| | 01010 | | Scan Profile 11 |
| | 01011 | | Scan Profile 12 |
| | 01100 | | Scan Profile 13 |
| | 01101 | | Scan Profile 14 |
| | 01110 | | Scan Profile 15 |
| | 01111 | | Scan Profile 16 |
| | 10000-11111 | | Undefined |

Table 4-7. Scanner Operations Flag Word 2 (of 3)

| Bit Position (Right to Left) | Bit Value | Detail Description | Meaning |
|---|---|---|---|
| 5-8 | | ES8-20-C | The last azimuth command is given below: |
| | 0000 | | Go To Position Crosstrack |
| | 0001 | | Go To Position A |
| | 0010 | | Go To Position B |
| | 0011 | | Go To Position Solar Calibration |
| | 0100 | | Go To Position Caged |
| | 0101 | | Go To Position Spare 1 |
| | 0110 | | Go To Position Spare 2 |
| | 0111 | | Go To Position Spare 3 |
| | 1000 | | Scan A B Asynchronously |
| | 1001 | | Scan A B Synchronously |
| | 1010 | | Stop Azimuth |
| | 1011-1111 | | Undefined |
| 9-11 | 000 | ES8-20-D | Normal Scan Operation |
| | 001 | | Initialization In Progress |
| | 010 | | At Initialized Position |
| | 011 | | Scan Abort In Progress |
| | 100 | | Elevation At Aborted Position |
| | 101-111 | | Undefined |
| 12-14 | 000 | ES8-20-E | Azimuth At Go To Position |
| | 001 | | Azimuth At Stopped Position |
| | 010 | | Azimuth At Initial Position |
| | 011 | | Azimuth At Scan Position |
| | 100 | | Azimuth In Motion |
| | 101-111 | | Undefined |
| 15 | 0 | | Instrument in Biaxial mode and azimuth is moving forward from $90^o$ toward $270^o$. |
| | 1 | | Instrument in Biaxial mode and azimuth is moving backward from $270^o$ toward $90^o$. |
| 16-31 | | | Spares |

See detail descriptions after Table 4-8.

Table 4-8. Scanner Operations Flag Word 3 (of 3)

| Bit Position (Right to Left) | Bit Value | Detail Description | Meaning |
|---|---|---|---|
| 0-1 | 00 | ES8-20-F | Instrument in FAPS Crosstrack (+/- $45^o$) Mode |
| | 01 | | Instrument in RAPS Mode |
| | 10 | | Instrument in FAPS Alongtrack (not crosstrack) Mode |
| | 11 | | Instrument in Transitional Mode |
| 2-31 | | | Spares |

**ES8-20-A Instrument Mode:**

**Instrument in Safe Mode:** The instrument is stowed during the safe mode for protection. If the solar presence sensors confirm the Sun is within the FOV of the sensors and that potential damage to the radiometers may result, the instrument will be automatically commanded to the Safe Mode.

**Instrument in Standby Mode:** The instrument is stowed during the Standby Mode.

**Instrument in Crosstrack Mode:** The azimuth is fixed to scan perpendicular to the satellite ground track. The elevation scan mode is either normal, short, or nadir scan (See ES8-20-B).

**Instrument in Biaxial Mode:** Both azimuth and elevation are operational. Azimuth rotation starts with the elevation scan plane in the along-track direction and rotates through 180 deg until the scan plane is again in the along-track direction, the process is then reversed. Azimuth rotation is continuous at a rate up to 6 deg $sec^{-1}$.

**Instrument in Solar Calibration Mode:** The instrument is oriented in azimuth and elevation to view the MAM.

**Instrument in Diagnostic Configuration Mode:** The instrument must be in the diagnostic mode to accept the following commands: scan table loads, internal command sequence loads, and special diagnostic loads.

**Instrument in Internal Calibration Mode:** Internal calibration is invoked by commands which control the blackbody sources and the SWICS. The scan profile is the same as Normal Earth Scan (See ES8-20-B) (Crosstrack Mode or Biaxial Mode) except that the blackbody heater and SWICS lamp are powered on. During internal calibration the instrument total and longwave sensors view the on-board blackbodies for calibration. The shortwave sensor views the SWICS. Internal calibrations are performed approximately every two weeks in orbit.

**Instrument in Special Short Scan Mode**

**Instrument in Contamination Safe Mode:** This mode is intended to minimize the modification of time tagged commands stored on board the spacecraft in the event a velocity maneuver is planned after the 24 hour command upload for the instruments is completed. The instrument will be stowed, all calibration sources turned off, the azimuth will be rotated to a safe position, and the instrument will remain in this mode for 10 minutes and then automatically go to the Standby Mode.

**Instrument in Hold Mode:** Same as Standby Mode above.

**Instrument in Abbreviated Internal Calibration Mode:** This mode is a similar to the Internal Calibration Mode with fewer sequences.

**Instrument in Fixed Azimuth Mode:** The azimuth is fixed at an angle (See ES8-20-F) to scan other than perpendicular to the satellite ground track (Crosstrack Mode). The exact azimuth angle is not included on the ES-8 product. The elevation scan profile is either Normal, Short, or Nadir Scan (See ES8-20-B).

**ES8-20-B Elevation Scan Profiles:**

**Stow**

**Normal Earth Scan:** The scan consists of scanning across the Earth. The sensor starts at space view, scans across the Earth, pauses at the opposite space look and slews up into the structure to view the (unpowered) internal calibration sources. The entire sequence is then reversed. The complete scan cycle is 6.6 sec in duration (See Term-13).

**Short Earth Scan:** The instrument goes into the short scan mode to protect the sensors from direct solar viewing if activated via ground command or the solar presence sensors. This mode is the same as the normal scan mode, except that the scan terminates 16 deg in elevation below the earth limb and begins rapid retrace (See Term-13) prior to the earth limb to avoid direct solar viewing. This mode is required only in the Biaxial Mode.

The Short Earth Scan assumes the Sun will only appear on one side of the satellite. The Sun is kept on one side by carefully choosing azimuth scan turn around points which are usually 180 deg apart, but under some conditions, the turn around points will be “pinched” (less than 180 deg apart) to make sure that the Sun remains on the “sun” side of the instrument.

**MAM Scan:** This scan profile is used during the Instrument Solar Calibration Mode. A nominal MAM scan starts with the sensors viewing space for a zero reference. The sensors are then rotated in elevation to view the MAM. The sensors are rotated back to space for another space look. Next the sensors are rotated to view the instrument’s internal calibration sources (blackbody and SWICS) and finally back to view space again. This cycle repeats every 6.6 sec.

**Nadir Scan:** During the nadir scan mode the scan pauses at nadir and then retraces to space look. This mode is used primarily during ground test and calibration.

**Scan Profile 6 through Scan Profile 16:** These profiles are programmable and used for special purposes at selected times.

**ES8-20-C Last Azimuth Command:**

**Go To Position Crosstrack:** The azimuth is rotated to the crosstrack position (See ES8-20-A) so that the scan is perpendicular to the satellite groundtrack.

**Go To Position A:** The azimuth is rotated to position A which is the starting position of the Biaxial Mode. The azimuth A is nominally in the forward alongtrack position, but is programmable to any value. The exact value of A is not included on the ES-8 product.

**Go To Position B:** The azimuth is rotated to position B which is the ending position of the Biaxial Mode. The azimuth B is nominally in the backward alongtrack position, but is programmable to any value. The exact value of B is not included on the ES-8 product.

**Go To Position Solar Calibration:** The azimuth is rotated to the position to view the MAM.

**Go To Position Caged:** The azimuth is rotated to the caged position.

**Go To Position Spare 1:** The azimuth is rotated to the spare 1 input position.

**Go To Position Spare 2:** The azimuth is rotated to the spare 2 input position.

**Go To Position Spare 3:** The azimuth is rotated to the spare 3 input position.

**Scan A B Asynchronously:** The azimuth is rotated to position A which is the starting position of the Biaxial Mode. When the azimuth reaches position A it then rotates to position B. This process is repeated until commanded otherwise.

**Scan A B Synchronously:** This is similar to the Scan A B Asynchronously command except in this command the instrument will synchronize the beginning of the 6.6 sec elevation scan cycle and the azimuth rotation cycle. The instrument will adjust the pause at the end of each azimuth cycle (at both A and B position) so that the cycles are always synchronized.

**Stop Azimuth:** The azimuth scan rate is immediately set to zero and the azimuth position held.

**ES8-20-D Scan Mode:**

**Normal Scan Operation**

**Initialization In Progress**

**At Initialized Position**

**Scan Abort In Progress**

**Elevation At Aborted Position**

**ES8-20-E Azimuth Position:**

**Azimuth At Go To Position**

**Azimuth At Stopped Position**

**Azimuth At Initial Position**

**Azimuth At Scan Position**

**Azimuth In Motion**

**ES8-20-F Azimuth Plane Position:**

**Instrument in FAPS Crosstrack (+/- 45$^{o}$) Mode:** The azimuth is fixed at a value within 45 deg of the perpendicular to the satellite groundtrack.

**Instrument in RAPS Mode:** The instrument is in the Biaxial Mode.

**Instrument in FAPS Alongtrack (not crosstrack) Mode**: The azimuth is fixed at a value greater than 45 deg from the perpendicular to the satellite groundtrack.

**Instrument in Transitional Mode:** The azimuth is in transition between modes.

## 4.4 Fill Values

Table 4-9 lists the default CERES Fill Values. Individual parameter definitions in the previous section explain how and when the default values are used. The CERES default fill values used on the ES-8 are defined as follows:

Table 4-9. CERES Fill Values

| Fill Value Name | Value | Fill Value Description* |
|---|---|---|
| INT4_DFLT | 2147483647 | default value for a 4-byte integer |
| REAL4_DFLT | 3.4028235E+38 | default value for a 4-byte real |
| REAL8_DFLT | 1.7976931348623157E+308 | default value for a 8-byte real |

## 4.5 Sample Data File

A sample data granule (See Term-9) containing 5 ES-8 records is part of a package which also includes sample read software (in C), a Readme file, a postscript file describing granule contents, and an ASCII listing of the data in the sample granule (data dump). The sample ES-8 package can be ordered from the Langley ASDC (See Section 12.0). It is available from the Langley ASDC Web Ordering Tool and has the name format: CERES_Test_ES8_version information.

# 5.0 Data Organization

Table 5-1 gives an overview of the ES-8 product. The metadata structures contain information which need only be recorded once per daily product. The CERES Baseline Header Metadata and the CERES_metadata Vdata are listed in Appendix A. As explained in Appendix A, the CERES Baseline Header Metadata includes either the bounding rectangle or GRing attributes. The spatial boundaries of the ES-8 are defined with the bounding rectangle. The ES-8 also contains Product Specific Metadata, which are shown in Table 5-2.

Table 5-1. ES-8 Product Summary

| HDF Name | Description | Number of Parameters | Nominal Size (MB) |
|---|---|---|---|
| CERES Baseline Header Metadata | See Table A-1 | 36 | |
| CERES_metadata Vdata | See Table A-2 | 14 | |
| ES-8 Product Specific Metadata | See Table 5-2 | 1 | |
| ES-8 Metadata Size (MB/Day) | | | 0.880 |
| ES-8 Vdata Summary | See Table 5-4 | 20 | 1.120 |
| ES-8 SDS Summary | See Table 5-3 | 20 | 467.108 |
| ES-8 Data Size (MB/Day) | | | 468.228 |
| **ES-8 Total Product Size (MB/Day)** | | | **469.087** |
| **ES-8 Total Product Size with HDF Data Compression** | | | **293.5[a]** |

a. GZIP Compression, Level 1

Table 5-2. ES-8 Product Specific Metadata

| Item | Parameter Name | Records | Units | Range | Data Type |
|---|---|---|---|---|---|
| 1 | ES8_ProductionDate | 1 | N/A | N/A | ASCII string |
| 2 | NumOfCrosstrackRecords | 1 | N/A | 0 .. 13092 | Integer |
| 3 | NumOfRAPSRecords | 1 | N/A | 0 .. 13092 | Integer |
| 4 | NumOfAlongtrackRecords | 1 | N/A | 0 .. 13092 | Integer |
| 5 | NumOfTransitionalRecords | 1 | N/A | 0 .. 13092 | Integer |
| 6 | Software_SCCR_Number | 1 | N/A | N/A | ASCII string |
| 7 | Data_SCCR_Number | 1 | N/A | N/A | ASCII string |

## 5.1 Data Granularity

All ES-8 HDF data granules consist of no more than 24 hours of data from one CERES instrument.

## 5.2 ES-8 HDF Scientific Data Sets (SDS)

The ES-8 contains 20 SDSs (See Term-19) which are 2-dimensional arrays of time ordered records where the first dimension corresponds to the number of data records contained in the data-day; the maximum is 13,092 (since the time length of a record may vary, the maximum number of records on the ES-8 can be 13,092). For the measurement-level data, other than flag words, the second dimension corresponds to the number of measurements or footprints contained on an individual data record (660). There are 22 measurement-level, 32-bit flag words that contain a flag value in each of the right-most 30 bits (22 words x 30 bits/word = 660 bits). For these measurement-level flag words, the second dimension is 22. See ES8-15 in 4.3.2 for a detailed explanation of the measurement-level flag words. Table 5-3 summarizes the content and size of each SDS contained within the ES-8 file. The Item identification given in the table for each parameter may be used to find the parameter descriptions in 4.3.2.

Table 5-3. ES-8 SDS Summary (1 of 2)

| Item | Parameter Name (SDS Name) | Units | Range | Maximum Number of SDS Elements | Data Type | Maximum SDS Size (MB) |
|---|---|---|---|---|---|---|
| ES8-1 | Colatitude of CERES FOV at TOA | deg | 0 .. 180 | 13092×660 | 32 bit real | 32.962 |
| ES8-2 | Longitude of CERES FOV at TOA | deg | 0 .. 360 | 13092×660 | 32 bit real | 32.962 |
| ES8-3 | CERES TOT filtered radiance | $W\ m^{-2}\ sr^{-1}$ | -2 .. 700 | 13092×660 | 32 bit real | 32.962 |
| ES8-4 | CERES SW filtered radiance | $W\ m^{-2}\ sr^{-1}$ | -4 .. 510 | 13092×660 | 32 bit real | 32.962 |
| ES8-5 | CERES WN filtered radiance | $W\ m^{-2}\ sr^{-1}\ \mu m^{-1}$ | -1 .. 15 | 13092×660 | 32 bit real | 32.962 |
| ES8-6 | CERES viewing zenith at TOA | deg | 0 .. 90 | 13092×660 | 32 bit real | 32.962 |
| ES8-7 | CERES solar zenith at TOA | deg | 0 .. 180 | 13092×660 | 32 bit real | 32.962 |
| ES8-8 | CERES relative azimuth at TOA | deg | 0 .. 360 | 13092×660 | 32 bit real | 32.962 |
| ES8-9 | CERES SW unfiltered radiance | $W\ m^{-2}\ sr^{-1}$ | -10 .. 510 | 13092×660 | 32 bit real | 32.962 |
| ES8-10 | CERES LW unfiltered radiance | $W\ m^{-2}\ sr^{-1}$ | 0 .. 200 | 13092×660 | 32 bit real | 32.962 |
| ES8-11 | CERES WN unfiltered radiance | $W\ m^{-2}\ sr^{-1}\ \mu m^{-1}$ | 0 .. 15 | 13092×660 | 32 bit real | 32.962 |
| ES8-12 | CERES SW flux at TOA | $W\ m^{-2}$ | 0 .. 1400 | 13092×660 | 32 bit real | 32.962 |
| ES8-13 | CERES LW flux at TOA | $W\ m^{-2}$ | 50 .. 450 | 13092×660 | 32 bit real | 32.962 |
| ES8-14 | ERBE scene identification at observation | N/A | 0 .. 12.4 | 13092×660 | 32 bit real | 32.962 |
| ES8-15 | TOT channel flag words | N/A | N/A | 13092×22 | 32 bit integer | 1.099 |
| ES8-16 | SW channel flag words | N/A | N/A | 13092×22 | 32 bit integer | 1.099 |
| ES8-17 | WN channel flag words | N/A | N/A | 13092×22 | 32 bit integer | 1.099 |

Table 5-3. ES-8 SDS Summary (2 of 2)

| Item | Parameter Name (SDS Name) | Units | Range | Maximum Number of SDS Elements | Data Type | Maximum SDS Size (MB) |
|---|---|---|---|---|---|---|
| ES8-18 | Scanner FOV flag words | N/A | N/A | 13092×22 | 32 bit integer | 1.099 |
| ES8-19 | Rapid retrace flag words | N/A | N/A | 13092×22 | 32 bit integer | 1.099 |
| ES8-20 | Scanner operations flag word | N/A | N/A | 13092×3 | 32 bit integer | 0.150 |
| **Total SDS Size** | | | | | | **467.11** |

## 5.3 ES-8 HDF Vertex Data (Vdata)

The ES-8 contains 20 record-level parameters written by HDF-EOS as HDF Vdata structures. These structures may be thought of as one-dimensional arrays dimensioned according to the number of data records contained in the data-day; the maximum is 13,092 (since the time length of a record may vary, the maximum number of records on the ES-8 can be 13,092). Each of these arrays contains one of the parameters listed in Table 5-4. The Item identification given in the table for each parameter may be used to find the parameter descriptions in 4.3.1.

Table 5-4. ES-8 Vdata Summary (1 of 2)

| Item | Parameter Name (Vdata Name) | Units | Range | Maximum Number of Vdata Elements | Data Type | Maximum Vdata Size (MB) |
|---|---|---|---|---|---|---|
| ES8-V1 | Time of observation | day | 2440000 .. 2480000 | 13092 | 64 bit real | 0.100 |
| ES8-V2 | Earth-Sun distance at record start | AU | 0.98 .. 1.02 | 13092 | 64 bit real | 0.100 |
| ES8-V3 | X component of satellite position at record start | m | $-8\times10^6$ .. $8\times10^6$ | 13092 | 32 bit real | 0.050 |
| ES8-V4 | X component of satellite position at record end | m | $-8\times10^6$ .. $8\times10^6$ | 13092 | 32 bit real | 0.050 |
| ES8-V5 | Y component of satellite position at record start | m | $-8\times10^6$ .. $8\times10^6$ | 13092 | 32 bit real | 0.050 |
| ES8-V6 | Y component of satellite position at record end | m | $-8\times10^6$ .. $8\times10^6$ | 13092 | 32 bit real | 0.050 |
| ES8-V7 | Z component of satellite position at record start | m | $-8\times10^6$ .. $8\times10^6$ | 13092 | 32 bit real | 0.050 |
| ES8-V8 | Z component of satellite position at record end | m | $-8\times10^6$ .. $8\times10^6$ | 13092 | 32 bit real | 0.050 |
| ES8-V9 | X component of satellite velocity at record start | m $sec^{-1}$ | $-1\times10^4$ .. $1\times10^4$ | 13092 | 32 bit real | 0.050 |
| ES8-V10 | X component of satellite velocity at record end | m $sec^{-1}$ | $-1\times10^4$ .. $1\times10^4$ | 13092 | 32 bit real | 0.050 |
| ES8-V11 | Y component of satellite velocity at record start | m $sec^{-1}$ | $-1\times10^4$ .. $1\times10^4$ | 13092 | 32 bit real | 0.050 |

Table 5-4. ES-8 Vdata Summary (2 of 2)

| Item | Parameter Name (Vdata Name) | Units | Range | Maximum Number of Vdata Elements | Data Type | Maximum Vdata Size (MB) |
|---|---|---|---|---|---|---|
| ES8-V12 | Y component of satellite velocity at record end | m $sec^{-1}$ | $-1\times10^4$ .. $1\times10^4$ | 13092 | 32 bit real | 0.050 |
| ES8-V13 | Z component of satellite velocity at record start | m $sec^{-1}$ | $-1\times10^4$ .. $1\times10^4$ | 13092 | 32 bit real | 0.050 |
| ES8-V14 | Z component of satellite velocity at record end | m $sec^{-1}$ | $-1\times10^4$ .. $1\times10^4$ | 13092 | 32 bit real | 0.050 |
| ES8-V15 | Colatitude of satellite nadir at record start | deg | 0 .. 180 | 13092 | 32 bit real | 0.050 |
| ES8-V16 | Colatitude of satellite nadir at record end | deg | 0 .. 180 | 13092 | 32 bit real | 0.050 |
| ES8-V17 | Longitude of satellite nadir at record start | deg | 0 .. 360 | 13092 | 32 bit real | 0.050 |
| ES8-V18 | Longitude of satellite nadir at record end | deg | 0 .. 360 | 13092 | 32 bit real | 0.050 |
| ES8-V19 | Colatitude of Sun at observation | deg | 0 .. 180 | 13092 | 32 bit real | 0.050 |
| ES8-V20 | Longitude of Sun at observation | deg | 0 .. 360 | 13092 | 32 bit real | 0.050 |
| ES8-V21 | Spectral Response Functions: | | | | | |
| | SW channel wavelengths | µm | 0 .. 200 | 632 | 32 bit real | 0.002 |
| | SW spectral response values | N/A | -1 .. 1 | 632 | 32 bit real | 0.002 |
| | TOT channel wavelengths | µm | 0 .. 200 | 1051 | 32 bit real | 0.004 |
| | TOT spectral response values | N/A | -1 .. 1 | 1051 | 32 bit real | 0.004 |
| | WN channel wavelengths | µm | 0 .. 200 | 871 | 32 bit real | 0.003 |
| | WN spectral response values | N/A | -1 .. 1 | 871 | 32 bit real | 0.003 |
| **Total Vdata Size** | | | | | | **1.12** |

## 5.4 ES-8 Metadata

The CERES metadata are listed in Table A-1 and Table A-2 in Appendix A. Table A-1 lists the CERES Baseline Header Metadata and Table A-2 lists the parameters in the Vdata Metadata Table. Note that the Vdata Metadata is a subset of the CERES Baseline Header Metadata.

# 6.0 Theory of Measurements and Data Manipulations

## 6.1 Theory of Measurements

See CERES ATBD Subsystem 2.0 (Reference 5).

## 6.2 Data Processing Sequence

The ERBE-like Inversion Subsystem (2.0) converts filtered radiometric measurements in engineering units received from the Instrument Subsystem (1.0) to instantaneous flux estimates at the TOA. This inversion process is dependent on several factors, including Earth surface features, the extent of cloudiness, and the relative geometry of the spacecraft, the sun, and the measurement FOV. Each radiometric measurement is spectrally corrected to give an unfiltered measurement. The observed scene is determined by a scene identification algorithm based on these unfiltered measurements, using angular distribution models and statistics provided by the CERES Science Team. Estimates of the radiant flux at the TOA are computed based on scene information, geometrical considerations, and the unfiltered measurements.

For detailed information see the ERBE-like Software Requirements Document (Subsystem 2.0) (Reference 6).

## 6.3 Special Corrections/Adjustments

Algorithms not discussed in the ATBD are discussed in this section.

## 7.0 Errors

See the Data Quality Summary {URL=http://eosweb.larc.nasa.gov/project/ceres/ES8/disclaimer_CER_ES8.html}.

## 7.1 Quality Assessment

QA activities are performed at the Science Computing Facility by the Data Management Team. Processing reports containing statistics and processing results are examined for anomalies. If the reports show anomalies, data visualization tools are used to examine those products in greater detail to begin the anomaly investigation. (See the QA flag description for this product.)

## 7.2 Data Validation by Source

See Subsystem 2.0 Validation Document (Reference 7) for details on the data validation plan.

# 8.0 Notes

Notes are given to expand on subjects that will help in the use and understanding of the ES-8 product. These notes are generally characterized by more details and longer length than other definitions (See Section 4.3).

## Note-1 Conversion of Julian Date to Calendar Date

The Julian Date is a time system that has been adopted by astronomers and is used in many scientific experiments. The Julian Date or Julian Day is the number of mean solar days since 1200 hours (GMT/UT/UTC/Zulu) on Monday, 24 November 4714 BCE, based on the current Gregorian calendar, or more precisely, the Gregorian Proleptic calendar. In other words, Julian day number 0 (zero) was Monday, 24 November 4714 BCE, 1200 hours (noon). A new Julian day starts when the mean Sun at noon crosses the Greenwich meridian. This differs from UT or Greenwich Mean Solar Time by 12 hours since UT changes day at Greenwich midnight. Table 8-1 below provides Julian day numbers which relate UT to Julian date.

Important facts related to the Gregorian calendar are:

a) There is no year zero; year -1 is immediately followed by year 1.

b) A leap year is any year which is divisible by 4, except for those centesimal years (years divisible by 100) which must also be divisible by 400 to be considered a leap year.

c) A leap year has 366 days, with the month of February containing 29 days.

d) Year -1 is defined as a leap year, thus being also defined as containing 366 days, and being divisible by 4, 100, and 400.

Information on history, calendars, and Julian day numbers can be found in Blackadar's "A Computer Almanac" (See Reference 8) and on the WWW (See Reference 9).

The Julian day whole number is followed by the fraction of the day that has elapsed since the preceding noon (1200 hours UTC). The Julian Date JDATE can be represented as:

JDATE = JDay + JFract

where:

JDay = the integer Julian Day number and
JFract = the "fractional" Julian day (0 to 0.99...9)
(e.g. 245_0814.0 = 1200 or noon, 31 December, 1997 UT)

When the fractional part of the combined Julian date is .0, it is noon or 1200 hours GMT and when the fraction part is .5, then it is midnight or 0000 hours GMT.

The calculation of GMT (YYYYMMDD-HH:MM:SS.SSS) from Julian date (JDATE) is performed using the following process.

1. The YYYYMMDD can be determined using Table 8-1 to find the year and the beginning of the month whose Julian Day occurs before the JDay integer value.

2. Calculate the number of days past the 0.5 day of the month via Table 8-1 which provides Julian day numbers which relate UT to Julian date.

The GMT is determined by first computing the number of seconds in the day since midnight:

```
if    JFract > 0.5,
then  Seconds = 86400.0 * (JFract-0.5)
if    JFract <= 0.5,
then  Seconds = 86400.0 * (JFract+0.5)
```

Then compute HH, MM, and SS where:

```
HH  =  Int(Seconds/3600)
MM  =  Int(Seconds-(HH*3600.0)/60)
SS  =  Seconds-(HH*60.0 + MM)*60.0
```

As an example, if JD = 244_5733.5833, then the GMT date is computed using Table 8-1 by finding the closest beginning monthly calendar noon date, which is Feb 0.5, 1984 (UT).

```
(Feb 0.5)      Jday
244_5731 < 244_5733.5833
```

JD = 244_5733.5833 is 2.5833 days past Feb 0.5, 1984 UT (i.e., past 1984 Jan $31^d$ $12^h$ $0^m$ $0^s$) where 1984 Jan $31^d$ $12^h$ $0^m$ $0^s$ = (244_5733-244_5731).

Beginning with the whole days portion of 2.5833 (i.e., 2), the GMT Date is
1984 Jan $31^d$ $12^h$ $0^m$ $0^s$ + 2 = 1984 Feb $2^d$ $12^h$ $0^m$ $0^s$.

Next, since JFract (0.5833) is > 0.5, $12^h$ is added to the GMT Date, yielding:
1984 Feb $2^d$ $12^h$ $0^m$ $0^s$ + $12^h$ $0^m$ $0^s$ = 1984 Feb $3^d$ $0^h$ $0^m$ $0^s$.

Finally, to get the GMT time and since JFract (0.5833) is > 0.5, the number of seconds = 86400 *(0.5833 -0.5) = 7197.12 yielding:

HH = 7197.12 / 3600 = 01.9992 = $01^h$

MM = 7197.12 - ((1*3600) / 60) = 59.952 = $59^m$

SS = 7197.12 - ((1*60) + 59)*60) = $57.12^s$

Therefore, the GMT Date corresponding to the Julian Date 244_5733.5833 =
1984 Feb $3^d$ $1^h$ $59^m$ $57.12^s$, which is UT = 1984 Jan $31^d$ $12^h$ $0^m$ $0^s$ + 2.5833 days.

Table 8-1. Julian Day Number

| Year | Jan 0.5[a] | Feb 0.5 | Mar 0.5 | Apr 0.5 | May 0.5 | June 0.5 | July 0.5 | Aug 0.5 | Sept 0.5 | Oct 0.5 | Nov 0.5 | Dec 0.5 |
|---|---|---|---|---|---|---|---|---|---|---|---|---|
| 1980t | 244_4239 | _4270 | _4299 | _4330 | _4360 | _4391 | _4421 | _4452 | _4483 | _4513 | _4544 | _4574 |
| 1981 | _4605 | _4636 | _4664 | _4695 | _4725 | _4756 | _4786 | _4817 | _4848 | _4878 | _4909 | _4939 |
| 1982 | _4970 | _5001 | _5029 | _5060 | _5090 | _5121 | _5151 | _5182 | _5213 | _5243 | _5274 | _5304 |
| 1983 | _5335 | _5366 | _5394 | _5425 | _5455 | _5486 | _5516 | _5547 | _5578 | _5608 | _5639 | _5669 |
| 1984t | _5700 | _5731 | _5760 | _5791 | _5821 | _5852 | _5882 | _5913 | _5944 | _5974 | _6005 | _6035 |
| 1985 | 244_6066 | _6097 | _6125 | _6156 | _6186 | _6217 | _6247 | _6278 | _6309 | _6339 | _6370 | _6400 |
| 1986 | _6431 | _6462 | _6490 | _6521 | _6551 | _6582 | _6612 | _6643 | _6674 | _6704 | _6735 | _6765 |
| 1987 | _6796 | _6827 | _6855 | _6886 | _6916 | _6947 | _6977 | _7008 | _7039 | _7069 | _7100 | _7130 |
| 1988t | _7161 | _7192 | _7221 | _7252 | _7282 | _7313 | _7343 | _7374 | _7405 | _7435 | _7466 | _7496 |
| 1989 | _7527 | _7558 | _7586 | _7617 | _7647 | _7678 | _7708 | _7739 | _7770 | _7800 | _7831 | _7861 |
| 1990 | 244_7892 | _7923 | _7951 | _7982 | _8012 | _8043 | _8073 | _8104 | _8135 | _8165 | _8196 | _8226 |
| 1991 | _8257 | _8288 | _8316 | _8347 | _8377 | _8408 | _8438 | _8469 | _8500 | _8530 | _8561 | _8591 |
| 1992t | _8622 | _8653 | _8682 | _8713 | _8743 | _8774 | _8804 | _8835 | _8866 | _8896 | _8927 | _8957 |
| 1993 | _8988 | _9019 | _9047 | _9078 | _9108 | _9139 | _9169 | _9200 | _9231 | _9261 | _9292 | _9322 |
| 1994 | _9353 | _9384 | _9412 | _9443 | _9473 | _9504 | _9534 | _9565 | _9596 | _9626 | _9657 | _9687 |
| 1995 | 244_9718 | _9749 | _9777 | _9808 | _9838 | _9869 | _9899 | _9930 | _9961 | _9991 | *0022 | *0052 |
| 1996t | 245_0083 | _0114 | _0143 | _0174 | _0204 | _0235 | _0265 | _0296 | _0327 | _0357 | _0388 | _0418 |
| 1997 | _0449 | _0480 | _0508 | _0539 | _0569 | _0600 | _0630 | _0661 | _0692 | _0722 | _0753 | _0783 |
| 1998 | _0814 | _0845 | _0873 | _0904 | _0934 | _0965 | _0995 | _1026 | _1057 | _1087 | _1118 | _1148 |
| 1999 | _1179 | _1210 | _1238 | _1269 | _1299 | _1330 | _1360 | _1391 | _1422 | _1452 | _1483 | _1513 |
| 2000t | 245_1544 | _1575 | _1604 | _1635 | _1665 | _1696 | _1726 | _1757 | _1788 | _1818 | _1849 | _1879 |
| 2001 | _1910 | _1941 | _1969 | _2000 | _2030 | _2061 | _2091 | _2122 | _2153 | _2183 | _2214 | _2244 |
| 2002 | _2275 | _2306 | _2334 | _2365 | _2395 | _2426 | _2456 | _2487 | _2518 | _2548 | _2579 | _2609 |
| 2003 | _2640 | _2671 | _2699 | _2730 | _2760 | _2791 | _2821 | _2852 | _2883 | _2913 | _2944 | _2974 |
| 2004t | 245_3005 | _3036 | _3965 | _3096 | _3126 | _3157 | _3187 | _3218 | _3249 | _3279 | _3310 | _3340 |
| 2005 | _3371 | _3402 | _3430 | _3461 | _3491 | _3522 | _3552 | _3583 | _3614 | _3644 | _3675 | _3705 |
| 2006 | _3736 | _3767 | _3795 | _3826 | _3856 | _3887 | _3917 | _3948 | _3979 | _4009 | _4040 | _4070 |
| 2007 | _4101 | _4132 | _4160 | _4191 | _4221 | _4252 | _4282 | _4313 | _4344 | _4374 | _4405 | _4435 |
| 2008t | 245_4466 | _4497 | _4526 | _4557 | _4587 | _4618 | _4648 | _5679 | _4710 | _4740 | _4771 | _4801 |
| 2009 | _4832 | _4863 | _4891 | _4922 | _4952 | _4983 | _5013 | _5044 | _5075 | _5105 | _5136 | _5166 |

[a] Jan. 0.5 (UT) is the same as Greenwich noon (12h) UT, Dec. 31. * These dates begin with 245 t Denotes leap years

## Note-2 Colatitude and Longitude of Nadir

The colatitude and longitude of the satellite nadir (See Term-11) at the start of the record are determined as follows. The position of the satellite is

x = (ES8-V3)

y = (ES8-V5)

z = (ES8-V7)

and the radius is $r = \sqrt{x^2 + y^2 + z^2}$ so that the colatitude (See Figure 4-1) is

$$\Theta = \cos^{-1}\left(\frac{z}{r}\right) \qquad 0° \le \Theta \le 180°$$

The projection of the radius on the equatorial plane is $r_{eq} = \sqrt{x^2 + y^2}$ so that the longitude is

$$\cos\Phi = \frac{x}{r_{eq}}$$

$$\sin\Phi = \frac{y}{r_{eq}}$$

$$\Phi = \tan^{-1}\left(\frac{\sin\Phi}{\cos\Phi}\right) \qquad 0° \le \Phi \le 360°$$

The colatitude and longitude at the end of the record is determined in a similar way with ES8-V4, ES8-V6, and ES8-V8.

# Note-3 CERES Point Spread Function

## Note-3.1 CERES Point Spread Function

The CERES scanning radiometer is an evolutionary development of the ERBE scanning radiometer. It is desired to increase the resolution as much as possible, using a thermistor bolometer as the detector. As the resolution is increased, the sampling rate must increase to achieve spatial coverage. When the sampling rate becomes comparable to the response time of the detector, the effect of the time response of the detector on the PSF must be considered. Also, the signal is usually filtered electronically prior to sampling in order to attenuate electronic noises and to remove high frequency components of the signal which would cause aliasing errors. The time response of the filter, together with that of the detector causes a lag in the output relative to the input radiance. This time lag causes the centroid of the PSF to be displaced from the centroid of the optical FOV. Thus, the signal as sampled comes not only from where the radiometer is pointed, but includes a “memory” of the input from where it had been looking. Another effect of the time response is to broaden the PSF, which will reduce the resolution of the measurement, increase blurring errors, and decrease aliasing errors.

## Note-3.2 Geometry of the Point Spread Function

The scanner footprint geometry is given in Figure 8-1. The optical FOV is a truncated diamond

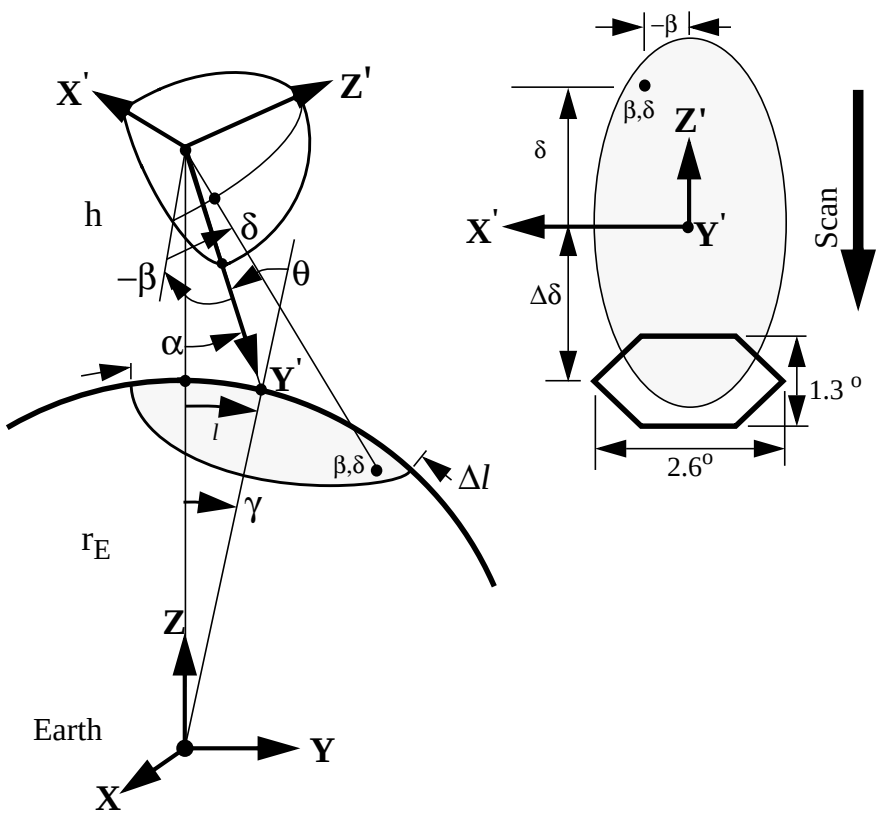


Figure 8-1. Scanner Footprint

(or hexagon) and is 1.3° in the along-scan direction and 2.6° in the across-scan direction. The effective FOV (or footprint) is given by the PSF and is shown as an ellipse. A point within the

footprint is located by β and δ. The cone angle α (or nadir angle) determines the location of the footprint centroid on the Earth. If α = 0, the footprint is at nadir. The viewing zenith angle θ is a direct result of the satellite altitude h, the Earth radius $r_E$, and the cone angle α. The surface distance $l$ and the Earth central angle γ between nadir and the centroid are also a result of the viewing geometry. In Figure 8-1 we have denoted the length of the FOV by $\Delta l$.

**Note-3.3 Analytic form of the Point Spread Function**

A full discussion of an analytic model of the point spread function and its development is given in Smith (See Reference 10). From Figure 8-1, we redraw half of the optical FOV in Figure 8-2

$$\delta'_f(\beta) = \begin{cases} -a & 0 \le \beta < a \\ -2a + \beta & a \le \beta < 2a \end{cases}$$

$$\delta'_b(\beta) = \begin{cases} a & 0 \le \beta < a \\ 2a - \beta & a \le \beta < 2a \end{cases}$$

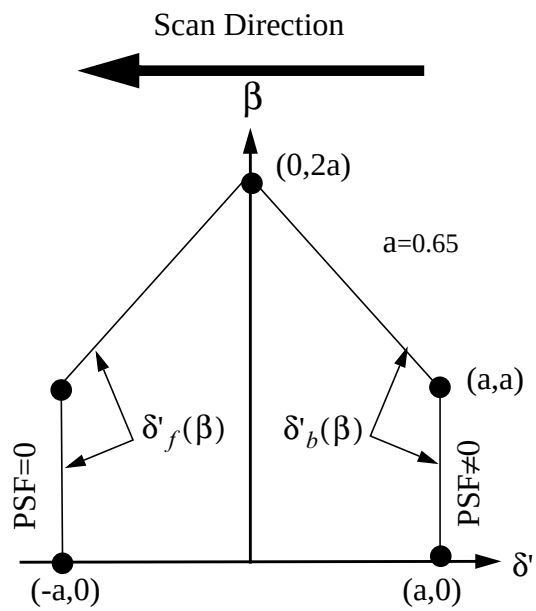


Figure 8-2. Optical FOV

where δ' is the along-scan angle and β is the cross-scan angle. Note that δ' points opposite the scan direction and increases toward the tail of the PSF (See Figure 8-3). The forward and back boundaries y and , respectively. With these definitions the CERES PSF are given by $\delta'_f(\beta)$ and $\delta'_b(\beta)$, respectively. With these definitions the CERES PSF is written as

$$P(\delta', \beta) = \begin{cases} 0 & |\beta| > 2a \\ 0 & \delta' < \delta'_f(\beta) \\ F[\delta' - \delta'_f(\beta)] & \delta'_f(\beta) \le \delta' < \delta'_b(\beta) \\ F[\delta' - \delta'_f(\beta)] - F[\delta' - \delta'_b(\beta)] & (otherwise) \end{cases} \quad (1)$$

where

$$
\begin{aligned}
F(\xi) \;=\; & 1-(1+a_1+a_2)e^{-1.78348\xi} \\
& + e^{-3.04050\xi}[a_1\cos(0.91043\xi)+b_1\sin(0.91043\xi)] \\
& + e^{-2.20860\xi}[a_2\cos(2.78981\xi)+b_2\sin(2.78981\xi)]
\end{aligned}
\tag{2}
$$

and

$$
a_1 = 5.83761 \qquad a_2 = -0.18956
$$
$$
b_1 = 2.87362 \qquad b_2 = 1.02431
$$

where $\xi$ is in degrees and $(0.91043\xi)$ and $(2.78981\xi)$ are in radians. The centroid of the PSF is derived in Smith (See Reference 10) and is $1.51^{o}$ from the optical axis. This shift is denoted in Figure 8-3 and a new angle $\delta$ is defined relative to the centroid. To evaluate the PSF we determine $\delta$ and then set $\delta' = \delta + \delta_0$ where $\delta_0$ is the shift (or offset) from the optical axis to the centroid.

The numerical values given in equation (1) are based on the following prelaunch calibration constants:

| | |
|---|---|
| $f_c = 10.5263$ hertz | Characteristic frequency of the Bessel Filter |
| $\tau = 0.0089$ sec | Detector time constant |
| $\dot{\alpha} = 63.0$ deg/sec | Scan rate |

Table must be from BDS - check for any text that goes with (currently no reference to Table 8-2)

Table 8-2. Detector Time Constant ($\tau$ seconds)

| Instrument | Detector Channel | | |
|---|---|---|---|
| | Total | Window | Shortwave |
| PFM | 0.00860 | 0.00830 | 0.00815 |
| FM1 | 0.00850 | 0.00795 | 0.00825 |
| FM2 | 0.00800 | 0.00820 | 0.00820 |
| FM3 | 0.00888 | 0.00868 | 0.00838 |
| FM4 | 0.00928 | 0.00858 | 0.00888 |

The general form of equation (1) is given by

$$
\begin{aligned}
F(\xi) \;=\; & 1-(1+a_1+a_2)e^{-\eta t} \\
& + e^{\mu_1 t}[a_1\cos(\omega_1 t)+b_1\sin(\omega_1 t)] \\
& + e^{\mu_2 t}[a_2\cos(\omega_2 t)+b_2\sin(\omega_2 t)]
\end{aligned}
\tag{3}
$$

where

$$t \;=\; \frac{2\pi f_c}{\dot{\alpha}}\,\xi$$

and where the complex roots of the 4-pole Bessel filter are

$$
\begin{aligned}
v_1 \;&=\; -2.89621 + 0.86723i \;=\; \mu_1 + i\omega_1 \\
v_2 \;&=\; -2.10379 + 2.65742i \;=\; \mu_2 + i\omega_2
\end{aligned}
$$

the residues of the Bessel filter are

$$
\begin{aligned}
u_1 \;&=\; +1.66339 - 8.39628i \\
u_2 \;&=\; -1.66339 + 2.24408i
\end{aligned}
$$

and

$$\eta \;=\; \frac{1}{2\pi f_c \tau}.$$

Note that $\omega_i$, $\eta$, and t are non-dimensional so that $(\omega_i t)$ is in radians. The cone angle $\xi$ has units of degrees. The complex variables $p_i$, $v_i$, $u_i$ define $a_i$ and $b_i$ as

$$p_i \;=\; \frac{u_i}{\eta + v_i}, \qquad a_i \;=\; 2\eta Re\left(\frac{p_i}{v_i}\right), \qquad b_i \;=\; -2\eta Imag\left(\frac{p_i}{v_i}\right), \qquad i \;=\; 1, 2$$

The centroid of the PSF can be derived from the analytic expression and is given by

$$\delta_0 \;=\; \dot{\alpha}\tau(1+\eta) \tag{4}$$

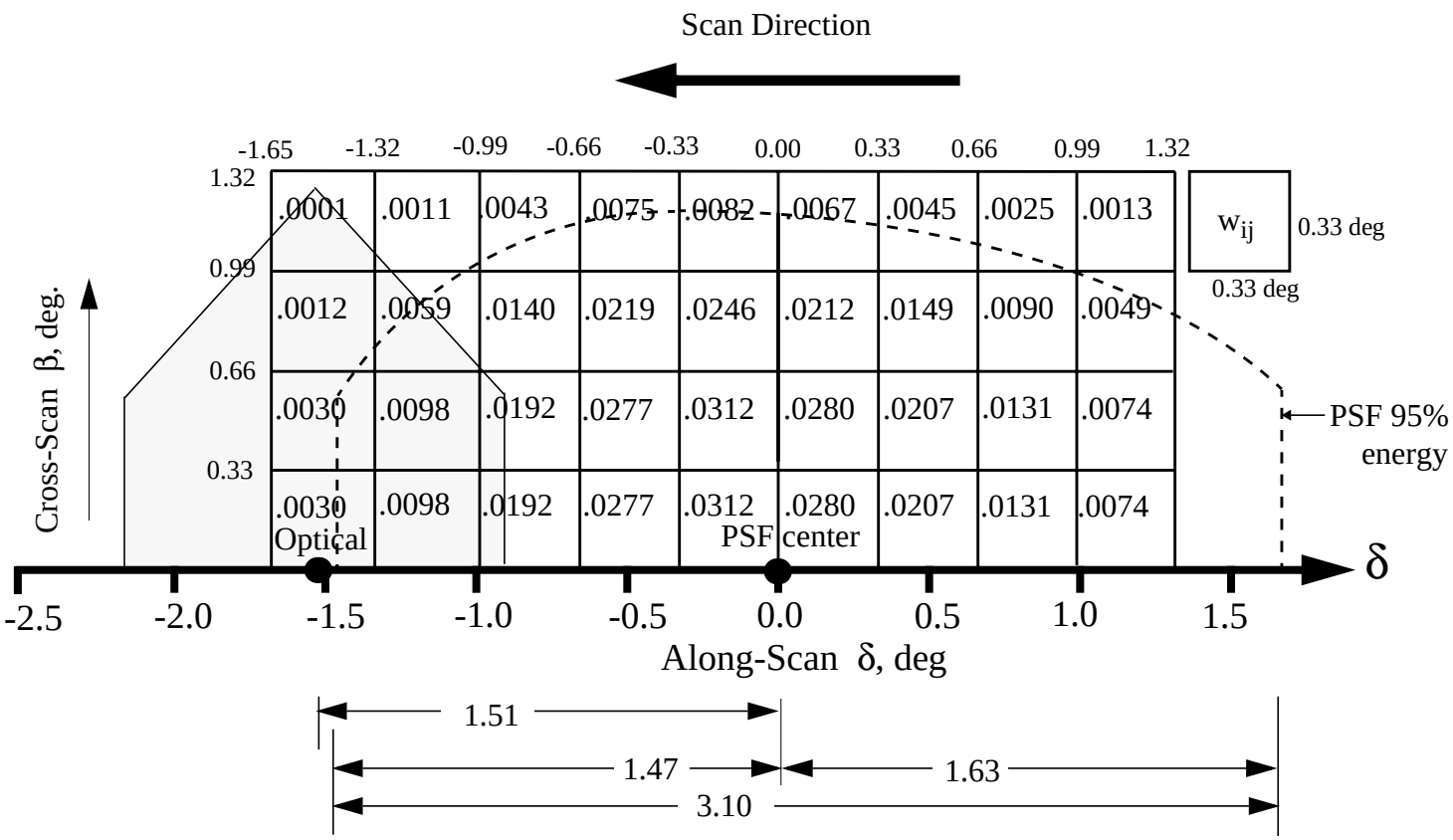


Figure 8-3. TRMM Angular Bin Weights

## Note-4 Definition of Angular Distribution Models (ADM)

The angular distribution model, $R(\theta, \phi)$, is a function of the viewing zenith angle, $\theta$, and relative azimuth angle, $\phi$, (See Figure 4-2) and defines the functional relationship between flux, F, and radiance, I, as

$$I(\theta, \phi) = \pi^{-1} F R(\theta, \phi) \tag{5}$$

Let us integrate radiance I in (5) over the hemisphere to get flux F, or

$$\int_0^{2\pi} \int_0^{\pi/2} I(\theta, \phi) \cos\theta \sin\theta d\theta d\phi = \pi^{-1} F \int_0^{2\pi} \int_0^{\pi/2} R(\theta, \phi) \cos\theta \sin\theta d\theta d\phi \tag{6}$$

or

$$\pi^{-1} \int_0^{2\pi} \int_0^{\pi/2} R(\theta, \phi) \cos\theta \sin\theta d\theta d\phi = 1 \tag{7}$$

which establishes a normalization for $R(\theta, \phi)$. It is common to assume R is independent of azimuth for longwave radiation so that the normalization (7) reduces to

$$2 \int_0^{\pi/2} R(\theta) \cos\theta \sin\theta d\theta = 1 \tag{8}$$

The main purpose for modeling anisotropy as $R(\theta, \phi)$ is to estimate flux from measured radiance by (5) as

$$\hat{F} = \frac{\pi^{-1} I(\theta, \phi)}{R(\theta, \phi)} \tag{9}$$

$R(\theta, \phi)$ is also a function of other angles and scene types such as land, ocean, cloud cover, optical depth, etc. For shortwave, $R_i(\theta, \phi; \theta_o)$ denotes R is a function of the solar zenith angle, $\theta_o$, (See Figure 4-2) and scene type i (See ES8-14). When constructing R from data, we sort the data into scene types and assume R is piecewise constant over angular bins. When evaluating R for specific angles $(\theta, \phi; \theta_o)$ we assume R is piecewise linear and use a tri-linear interpolation and a slightly different normalization constant. There is no interpolation between scene types. For longwave, $R_i(\theta; \Theta)$ denotes R is a function of colatitude, $\Theta$, and scene type i. Construction and evaluation is the same as for shortwave.

## Note-5 Maximum Likelihood Estimator (MLE) of Scene Type

The Maximum Likelihood Estimator (MLE) is a bi-spectral identifier of cloud cover where clouds are characterized as cold and bright. Based on the unfiltered shortwave and longwave scanner measurements

$$I^{SW} = (\text{ES8-9})$$

$$I^{LW} = (\text{ES8-10})$$

the scene corresponding to each scanner measurement is identified as one of four cloud conditions over a predetermined geographic or surface type. The first step is to determine the 2.5° region that contains the scanner TOA point (See Term-23) given by ES8-1 and ES8-2. From a priori physical data, we then determine the geographic scene as either ocean, land, snow, desert, or land-ocean mix. Next we determine the cloud condition. An example of a typical scene identification is shown in Figure 8-4.

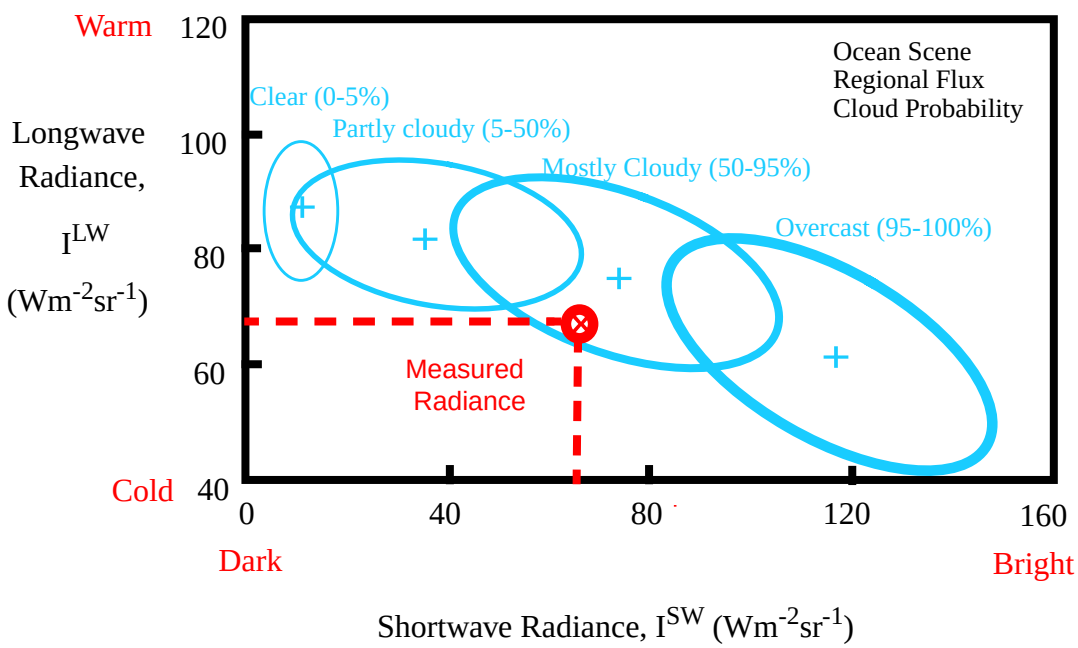


Figure 8-4. ERBE Scene Identification Algorithm

Knowing the geographic scene and the directional angles ES8-6, ES8-7, and ES8-8, we can evaluate from a priori data the measurements we would expect from a clear sky, partly cloudy, mostly cloudy, and overcast conditions. The ellipse about each point represents the variance we would expect. The identification consists of determining which one of the four cloud conditions is the closest to the actual measurement point in a probabilistic sense. The details of the MLE are given by Wielicki and Green (Reference 12).

## Note-6 Spectral Correction Algorithm

The radiances as measured by the CERES instruments are filtered radiances and the spectral correction algorithm unfilters these radiances. The desired unfiltered radiances are defined by

$$I^{SW} = \int_0^\infty I_\lambda^r d\lambda$$

$$I^{LW} = \int_0^\infty I_\lambda^e d\lambda$$

$$I^{WN} = \frac{1}{\lambda_2 - \lambda_1}\int_{\lambda_1}^{\lambda_2} I_\lambda^e d\lambda$$

where $\lambda$ (μm) is the wavelength, $\lambda_1 = 8.1$ and $\lambda_2 = 11.8$, and $I_\lambda^r$ and $I_\lambda^e$ are the reflected and emitted components of the total observed radiance or $I_\lambda = I_\lambda^r + I_\lambda^e$. The filtered measurements are modeled as

$$m_f^i = \int_0^\infty S_\lambda^i I_\lambda d\lambda \qquad i = \text{SW, TOT}$$

$$m_f^i = \frac{1}{\lambda_2 - \lambda_1}\int_0^\infty S_\lambda^i I_\lambda d\lambda \qquad i = WN$$

where $S_\lambda^i$ is the normalized spectral response function $(0 \le S_\lambda^i \le 1)$. The spectral response function for CERES_ TRMM is shown in the Figure 8-5 and represents the spectral throughput of the individual detector's optical elements determined from laboratory measurements. An estimate of the unfiltered SW and WN radiances are determined from the filtered radiance measurements as follows:

$$\hat{I}^{SW} = a_0 + a_1 (m_f^{SW_r}) + a_2 (m_f^{SW_r})^2$$

$$\hat{I}^{WN} = b_0 + b_1 (m_f^{WN}) + b_2 (m_f^{WN})^2$$

where $a_0$, $a_1$, $a_2$, $b_0$, $b_1$, and $b_2$ are theoretically derived regression coefficients that depend on scene type and viewing geometry. $m_f^{SW_r}$ represents the reflected portion of the filtered SW radiance measurement and is given by $m_f^{SW_r} = m_f^{SW} - m_f^{SW_e}$ where $m_f^{SW_e}$ is the emitted thermal portion of $m_f^{SW}$ and is estimated from $m_f^{WN}$ using a pre-determined empirical 2nd order polynomial expression relating nighttime $m_f^{SW}$ and $m_f^{WN}$ measurements. For CERES_ TRMM the least-square fit is given by:

$$m_f^{SW_e} = k_0 + k_1(m_f^{WN}) + k_2(m_f^{WN})^2$$

where $k_0$ = 0.1208, $k_1$ = -0.001697, and $k_2$ = 0.0006875. Since there are no filtered longwave radiance measurements in CERES, the unfiltered emitted LW radiance must be inferred from measurements in the other available channels. An estimate of the daytime (D) and nighttime (N) LW radiance is given by

$$\hat{I}^{LW}(D) = c_0 + c_1 m_f^{SW_r} + c_2 m_f^{TOT} + c_3 m_f^{WN}$$

$$\hat{I}^{LW}(N) = d_0 + d_1 m_f^{TOT} + d_2 m_f^{WN}$$

where the c and d coefficients are theoretically derived regression coefficients. All of the spectral correction coefficients (SCC) are obtained from a regression analysis of theoretically derived filtered and unfiltered radiances in each channel. The simulated radiances are inferred from a spectral radiance database of typical Earth scenes and the spectral response functions. Each CERES instrument has its own set of SCC based on its spectral response. There are different SCC for land, ocean, snow, and cloud. The SCC also vary with solar zenith, viewing zenith, and relative azimuth. Additional details are given in Reference 13.

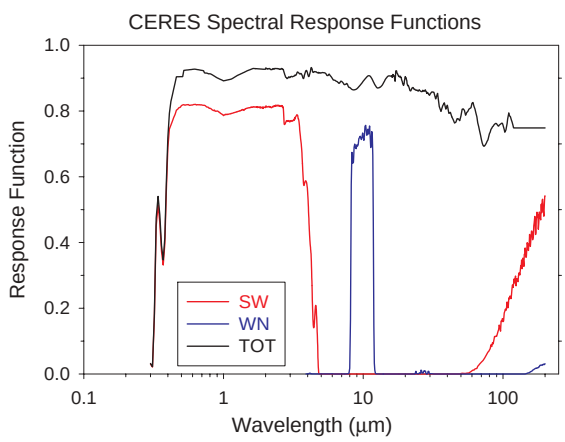


Figure 8-5. CERES_TRMM Spectral Response

## 9.0 Application of the Data Set

The ES-8 data product provides time and position data on a record-level basis and measurement-level data including filtered, unfiltered, TOA, and scene identification data (See Section 1.4).

## 10.0 Future Modifications and Plans

Modifications to the ES-8 product are driven by validation results and any Terra related parameters. The Langley ASDC provides users notification of changes.

## 11.0 Software Description

There are Fortran90 and C read programs available at the Langley ASDC. The programs were designed to run on a Unix workstation and can be compiled with a Fortran90 or C compiler, respectively.
*{Pointer to ASDC read program}*

## 12.0 Contact Data Center/Obtain Data

NASA Langley Atmospheric Sciences Data Center
Science, User and Data Service Office
NASA Langley Research Center
Mail Stop 157D
2 South Wright Street
Hampton, VA 23681-2199
USA

Telephone: (757) 864-8656
FAX: (757) 864-8807
E-mail: larc@eos.nasa.gov
URL: http://eosweb.larc.nasa.gov/

## 13.0 Output Products and Availability

Several media types are supported by the Langley Web Order Tool. Data can be downloaded from the Web or via FTP. Alternatively, data can be ordered on media tapes. The media tapes supported are 4mm 2Gb (90m), 8mm 2Gb (8200), 8mm 5Gb (8500), and 8mm 7Gb (8500c).

Data ordered via the Web or via FTP can be downloaded in either Uncompressed mode or in UNIX Compressed mode. Data written to media tape (in either Uncompressed mode or in UNIX Compressed mode) is in UNIX TAR format.

## 14.0 References


1. NASA Langley Atmospheric Science Data Hierarchical Data Format Web site {URL = http://eosweb/HBDOCS/hdf.html}.
2. Clouds and the Earth's Radiant Energy System (CERES) Data Management System Data Products Catalog Release 3, Version 1, July 1998 {URL = http://asd-www.larc.nasa.gov/DPC/DPC.html}.
3. TRW DRL 64, 55067.300.008E; In-flight Measurement Analysis (Rev. E), March 1997.
4. Clouds and the Earth's Radiant Energy System (CERES) Algorithm Theoretical Basis Document, Instrument Geolocate and Calibrate Earth Radiances (Subsystem 1.0), Release 2.2, June 1997 {URL = http://asd-www.larc.nasa.gov/ATBD/ATBD.html}.
5. Clouds and the Earth's Radiant Energy System (CERES) Algorithm Theoretical Basis Document, ERBE-like to Instantaneous Fluxes (Subsystem 2.0), Rel. 2.2, June 2, 1997 {URL = http://asd-www.larc.nasa.gov/ATBD/ATBD.html}.
6. Clouds and the Earth's Radiant Energy System (CERES) Data Management System Software Requirements Document, ERBE-like Inversion to Instantaneous TOA and Surface Fluxes (Subsystem 2.0), Release 1 Version 1, November 1994 {URL = http://asd-www.larc.nasa.gov/SRD/SRD.html}.
7. Clouds and the Earth's Radiant Energy System (CERES) Validation Plan, ERBE-like Inversion to Instantaneous TOA Flux (Subsystem 2.0), Release 2.2, July 1997 {URL = http://asd-www.larc.nasa.gov/validation/valid_doc.html}
8. Blackadar, Alfred: A Computer Almanac, Weatherwise, Vol 37, No 5, October 1984, p. 257-260.
9. Jefferys, William H.: Julian Day Numbers {URL = http://quasar.as.utexas.edu/BillInfo/JulianDatesG.html}.
10. Smith, G. L., 1994: Effects of time response on the point spread function of a scanning radiometer, Appl. Opt., Vol. 33, No. 30, 7031-7037.
11. Software Bulletin "CERES Metadata Requirements for LaTIS," Revision 1, January 7, 1998 {URL = http://asd-www.larc.nasa.gov/ceres/bulletins.html}.
12. Wielicki, B. A., and R. N. Green, 1989: Cloud identification for ERBE radiation flux retrieval, *J. Appl. Meteor.*, **28**, 1133-1146.
13. Loeb, N. G., Priestley, K. J., Kratz, D. P., Geier, E. B., Green, R. N., Wielicki, B. A., Hinton, P. O'R., and Nolan, S. K.: Determination of Unfiltered Radiances from CERES. Submitted to Journal of Applied Meteorology, 2000.

# 15.0 Glossary of Terms

### Term-1 Cone Angle

The cone angle (See Figure 15-1) is the angle between a vector from the satellite to the center of the Earth and the instrument view vector from the satellite to the TOA point (See Term-23).

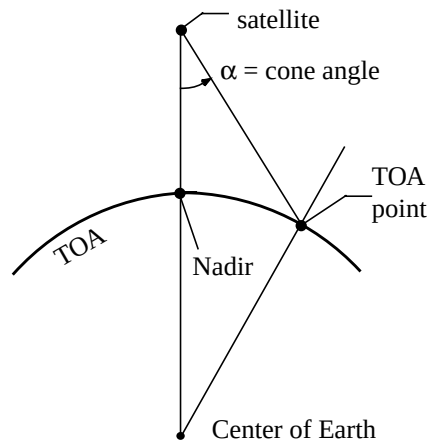


Figure 15-1. Cone Angle

### Term-2 Count Conversion

Conversion from instrument counts to engineering units by a count conversion equation (See Reference 4 and BDS Collection Guide, Note 1).

### Term-3 Earth Equator, Greenwich Meridian System

The Earth equator, Greenwich meridian system is an Earth-fixed, geocentric, rotating coordinate system with the X-axis in the equatorial plane through the Greenwich meridian, the Y-axis lies in the equatorial plane $90^o$ to the east of the X-axis, and the Z-axis is toward the North Pole.

### Term-4 Earth Surface

The surface of the Earth as defined by the WGS-84 Earth Model. The WGS-84 model of the Earth surface is an ellipsoid

$$\frac{x^2}{a^2} + \frac{y^2}{a^2} + \frac{z^2}{b^2} = 1 \text{ where}$$

a = 6378.1370 km and
b = 6356.7523 km (See Figure 15-2). We can determine the radial distance r as a function of the geocentric latitude θ by setting x = r cos(θ), y = 0, z = r sin(θ) in the ellipsoidal model and solving for r

$$\text{or } r = \frac{ab}{\sqrt{a^2 \sin^2\theta + b^2 \cos^2\theta}}$$

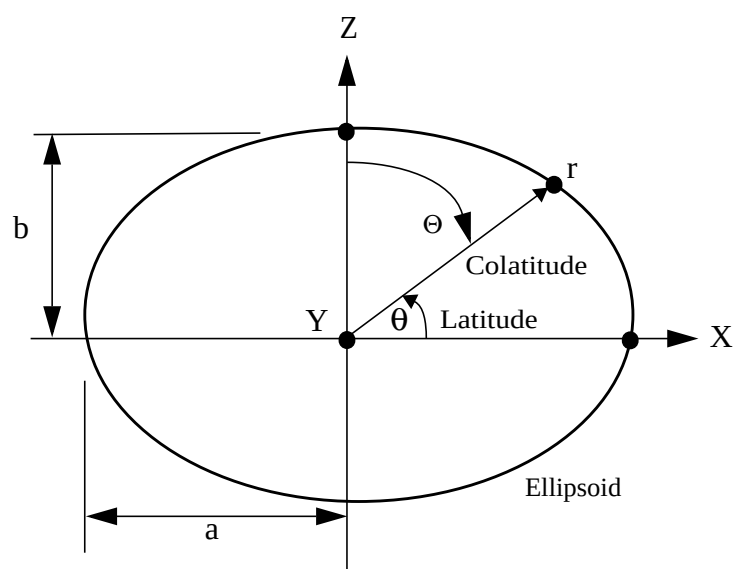


Figure 15-2. Ellipsoidal Model

### Term-5 Elevation Angle

The elevation angle defines the position of the instrument optical axis (See Note-3) relative to the spacecraft. For nominal satellite attitude control, the elevation is near $90^o$ for a nadir view (See Term-11), near $0^o$ at the start of a 6.6 sec scan cycle, and near $180^o$ at internal calibrations. Zero elevation is generally away from the Sun and $180^o$ is generally on the sun side of the satellite.

**Term-6 Field-of-View**

The instrument field-of-view (FOV) is determined by the instrument point spread function (See Term-12) and is defined as the minimum area over the radiation field from which 95% of the measured radiance is obtained. For the purpose of determining full FOV coverage of the Earth surface (See ES8-18), the forward edge of the FOV is offset 1.7 deg at the satellite in front of the PSF centroid while the trailing edge is offset 1.7 deg behind the centroid. (See Note-3).

**Term-7 Fixed azimuth plane scan (FAPS)**

**Term-8 Geocentric Colatitude**

**Term-9 Granule**

The ES-8 product is one day or 24 hours of data and is called a granule. Or, a granule is all records (See Term-14) for a day.

**Term-10 Julian Date**

Julian Date is a continuous count of time in whole and fractional days elapsed at the Greenwich meridian since noon on January 1, 4714 BCE. (See Note-1)

**Term-11 Nadir**

The point on the Earth surface below the satellite or the intersection point of a line from the center of the Earth to the satellite and the Earth surface (See Figure 15-1).

**Term-12 Point Spread Function**

A Point Spread Function (PSF) is a two-dimensional bell-shaped function that defines the CERES instrument response to the viewed radiation field. Due to the response time, the radiometer responds to a larger FOV than the optical FOV and the resulting PSF centroid lags the optical FOV centroid by more than a degree of cone angle (See Term-1) for normal scan rates (See Note-3).

**Term-13 Rapid Retrace (or Fast Return)**

Rapid retrace is defined as a much faster than nominal elevation, or cone angle, scan rate. The rapid retrace rate is currently defined as 249.69 10 deg $sec^{-1}$. During the Short Elevation Scan cycle, there are two portions of the scan cycle where the CERES instrument sweeps across the Earth at a rate of approximately 249 deg $sec^{-1}$. These are examples of rapid retrace (See Figure 15-3).

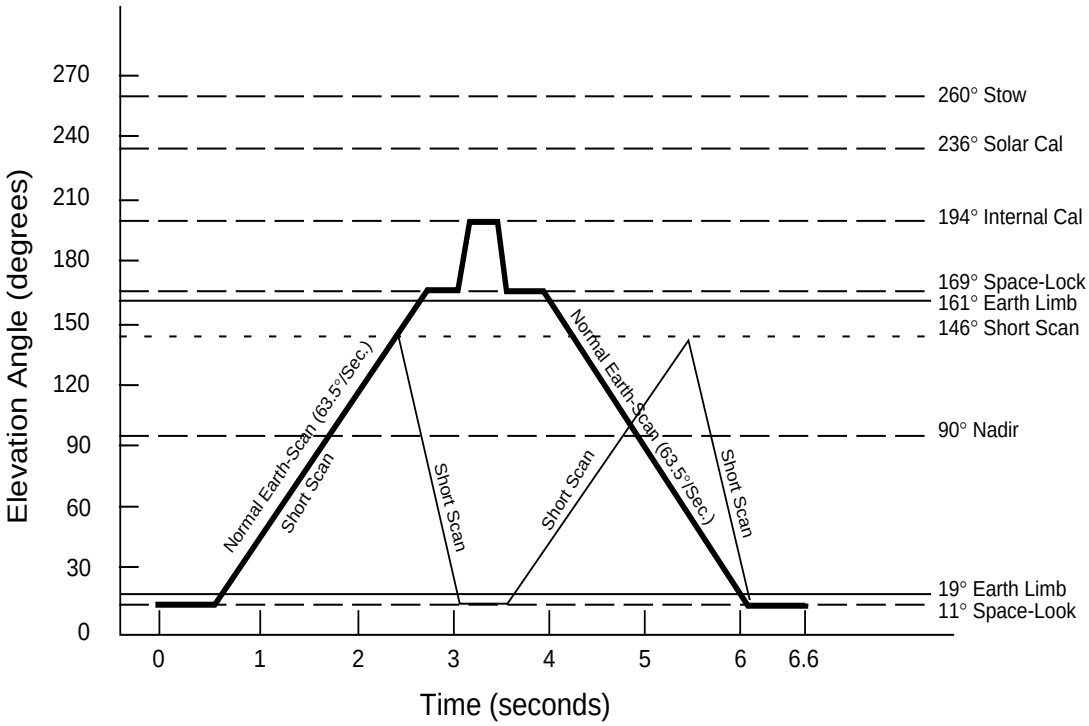


Figure 15-3. Normal and short Earth scan profiles for instrument on TRMM platform

### Term-14 Record

A record contains data from one complete scan cycle of 6.6 sec (See Term-17). The records are ordered and numbered in time from 1 to a maximum of 13,092 (note: since the time length of a record may vary, the maximum number of records on the ES-8 can be 13,092). The record number is one of the dimension indices of the HDF output arrays.

### Term-15 Resolution

### Term-16 Rotation Azimuth Plane Scan (RAPS)

### Term-17 Scan Cycle

Each scan cycle is 6.6 sec in length and contains 660 measurement points so that measurements are every 0.01 sec. The beginning of a scan cycle is at measurement 1. The end of a cycle is 6.6 sec later at measurement 1 of the next cycle. The last measurement in the scan cycle is 660 and is 6.59 sec after measurement 1.

### Term-18 Scan Sample Number

Each of the 660 measurements or samples within a scan cycle (See Term-17) is ordered and numbered in time from 1 to 660. The scan sample number is also one of the dimension indices of the HDF output arrays.

### Term-19 Scientific Data Set

A Scientific Data Set (SDS) is an HDF structure. It is a collection (or grouping) of parameters that have the same data type such as 8, 16, or 32-bit integers or 32, or 64-bit floating point numbers. The ES-8 SDS's each contain only one parameter. The SDS is an array of values and for ES-8 this corresponds to a two dimensional array of all values of a certain parameter for a day. The dimensions of the array correspond to the number of footprints (660) within a record (scan cycle) and the number of records within the granule. In general, an SDS is a multi-dimensional array. It has dimension records and data type which describe it. The dimensions specify the shape and size of the SDS array. Each dimension has its own attributes.

### Term-20 Spectral Correction

The Spectral Correction Coefficients (SCC) represent a regression between theoretical filtered radiances and theoretical unfiltered radiances and are used to unfilter the CERES radiances. Each CERES instrument has its own set of SCC based on its spectral response. There are different SCC for land, ocean, snow, and cloud. The SCC also vary with solar zenith, viewing zenith, and relative azimuth. (See Note-6)

### Term-21 Subsolar Point

The point at which a vector from the center of the Earth to the Sun intersects the TOA (See Term-22).

### Term-22 Top-of-the-Atmosphere

The Top-of-the-Atmosphere (TOA) is a surface approximately 30 km above the Earth surface (See Term-4). Specifically, the TOA is an ellipsoid $\frac{x^2}{a^2} + \frac{y^2}{a^2} + \frac{z^2}{b^2} = 1$ where a = 6408.1370 km and b = 6386.6517 km (See Figure 15-2). We can determine the radial distance r as a function of the geocentric latitude $\theta_c$ by setting x = r cos(θ), y = 0, z = r sin(θ) in the ellipsoidal model and solving for r or

$$r = \frac{ab}{\sqrt{a^2 \sin^2\theta + b^2 \cos^2\theta}}$$

### Term-23 TOA Point

The viewed point at the TOA, or the point at which the PSF (See Term-12) centroid intersects the TOA (See Term-22).

### Term-24 Vertex Data

A Vertex data (Vdata) set is an HDF structure. It is a collection (or grouping) of parameters that have different data types such as 8, 16, or 32-bit integers, floating point numbers, text, etc. In general, Vdata is a table of parameters of varying data type. Specifically stated, a Vdata is a customized table, comprised of a collection of similar records (rows) whose values are stored in

one or more fixed length fields (columns) where individual fields can have their own data type. The ES-8 contains 20 record-level parameters, each of which is written into a separate Vdata. Therefore, an ES-8 record-level Vdata contains a single field (column) which has multiple values (rows) such that one value exists for each record (scan cycle) within the granule. The ES-8 also contains a CERES_metadata Vdata which contains numerous parameters (columns) and each parameter has only one value per granule. A Vdata is uniquely identified by a name, a class, and individual field names. The Vdata class identifies the purpose or use of its data.

# 16.0 Acronyms and Units

## 16.1 CERES Acronyms

| | |
|---|---|
| ADM | Angular Distribution Model |
| APID | Application Identifier |
| APD | Aerosol Profile Data |
| ATBD | Algorithm Theoretical Basis Document |
| AVG | Monthly Regional Radiative Fluxes and Clouds |
| AVHRR | Advanced Very High Resolution Radiometer |
| BCE | Before Current Era |
| BDS | BiDirectional Scan (data product) |
| CADM | CERES Angular Distribution Model |
| CER | CERES |
| CERES | Clouds and the Earth's Radiant Energy System |
| CID | Cloud Imager Data (data product) |
| CRH | Clear Reflectance History (data product) |
| CRS | Clouds and Radiative Swath (data product) |
| CW | Cable Wrap |
| DAAC | Distributed Active Archive Center |
| DAC | Digital to Analog Converter |
| DAO | Data Assimilation Office |
| DAP | Data Acquisition microProcessor |
| DMA | Direct Memory Access |
| DMS | Data Management System |
| DPC | Data Products Catalog |
| ECR | Earth-Centered Rotating |
| EDDB | ERBE-Like Daily Database Product |
| EDOS | EOS Data Operations System |
| EOS | Earth Observing System |
| EOS AM | EOS Morning Crossing Mission (Renamed Terra) |
| EOS PM | EOS Afternoon Crossing Mission (Renamed Aqua) |
| EOSDIS | Earth Observing System Data and Information System |
| ERBE | Earth Radiation Budget Experiment |
| ERBS | Earth Radiation Budget Satellite |
| FAPS | Fixed Azimuth Plane Scan |

| | |
|---|---|
| FM | Flight Model |
| FOV | Field-of-View (See Term-6) |
| FSW | Monthly Single Satellite Fluxes and Clouds |
| FTP | File Transfer Protocol |
| GAP | Gridded Analysis Product |
| GB | Gigabyte |
| GEO | Geostationary Narrowband Radiances |
| GMS | Geostationary Meteorological Satellite |
| GGEO | Gridded Geostationary Narrowband Radiances |
| GMT | Greenwich Mean Time |
| GOES | Geostationary Operational Environmental Satellite |
| H | High |
| HDF | Hierarchical Data Format |
| IES | Instrument Earth Scans (data product) |
| IGBP | International Geosphere Biosphere Programme |
| INSTR | Instrument |
| ISCCP | International Satellite Cloud Climatology Project |
| IWC | Ice Water Content |
| LaRC | Langley Research Center |
| LaTIS | Langley TRMM Information System |
| L | Low |
| LM | Lower Middle |
| LW | Longwave |
| LWC | Liquid Water Content |
| MAM | Mirror Attenuator Mosaic |
| MB | Megabyte |
| METEOSAT | Meteorological Satellite |
| MISR | Multi-angle Imaging SpectroRadiometer |
| MLE | Maximum Likelihood Estimator |
| MOA | Meteorological, Ozone, and Aerosols (data product) |
| MODIS | Moderate Resolution Imaging Spectrometer |
| MWH | Microwave Humidity (data product) |
| NASA | National Aeronautics and Space Administration |
| NOAA | National Oceanic and Atmospheric Administration |
| OPD | Ozone Profile Data (data product) |
| PFM | Prototype Flight Model (on TRMM) |
| PSA | Product Specific Attribute |
| PSF | Point Spread Function (See Term-12) |
| QA | Quality Assessment |
| RAPS | Rotating Azimuth Plane Scan |
| SARB | Surface and Atmospheric Radiation Budget |
| SBUV-2 | Solar Backscatter Ultraviolet/Version 2 |
| SDS | Scientific Data Set (See Term-19) |
| SFC | Hourly Gridded Single Satellite TOA/Surface Fluxes and Clouds (data product) |
| SPS | Solar Presence Sensor |
| SRB | Surface Radiation Budget |

| | |
|---|---|
| SRBAVG | Surface Radiation Budget Average (data product) |
| SS | Subsystem |
| SSF | Single Satellite CERES Footprint TOA and Surface Fluxes, Clouds (data product) |
| SSM/I | Special Sensor Microwave/Imager |
| SURFMAP | Surface Map |
| SW | Shortwave |
| SWICS | Shortwave Internal Calibration Source |
| SYN | Synoptic Radiative Fluxes and Clouds |
| TBD | To Be Determined |
| TISA | Time Interpolation and Spatial Averaging |
| TMI | TRMM Microwave Imager |
| TOA | Top-of-the-Atmosphere (See Term-22) |
| TOT | Total |
| TRMM | Tropical Rainfall Measuring Mission |
| UM | Upper Middle |
| URL | Uniform Resource Locator |
| UT | Universal Time |
| UTC | Universal Time Code |
| VIRS | Visible Infrared Scanner |
| WN | Window |
| WWW | World Wide Web |
| ZAVG | Monthly Zonal and Global Average Radiative Fluxes and Clouds (data product) |

## 16.2 CERES Units

### Unit Definitions

| Units | Definition |
|---|---|
| AU | Astronomical Unit |
| cm | centimeter |
| count | count, counts |
| day | day, Julian date |
| deg | degree |
| deg $sec^{-1}$ | degrees per second |
| du | Dobson units |
| fraction | fraction 0..1 |
| g $kg^{-1}$ | gram per kilogram |
| g $m^{-2}$ | gram per square meter |
| hhmmss | hour, minute, second |
| hour | hour |
| hPa | hectoPascals |

| Units | Definition |
|---|---|
| in-oz | inch-ounce |
| K | Kelvin |
| km | kilometer, kilometers |
| km $sec^{-1}$ | kilometers per second |
| m | meter |
| mA | milliamp, milliamps |
| micron | micrometer, micron |
| msec | millisecond |
| mW $cm^{-2}sr^{-1}\mu m^{-1}$ | milliWatts per square centimeter per steradian per micron |
| m $sec^{-1}$ | meter per second |
| N/A | not applicable, none, unitless, dimensionless |
| percent | percent, percentage 0..100 |
| rad | radian |
| sec | second |
| volt | volt, volts |
| W h $m^{-2}$ | Watt hour per square meter |
| $W^2$ $m^{-4}$ | square Watt per meter to the 4th |
| W $m^{-2}$ | Watt per square meter |
| W $m^{-2}sr^{-1}$ | Watt per square meter per steradian |
| W $m^{-2}sr^{-1}\mu m^{-1}$ | Watt per square meter per steradian per micron |
| °C | degrees centigrade |
| µm | micrometer, micron |

# 17.0 Document Information

## 17.1 Document Creation Date - May 15, 1998

## 17.2 Document Review Date -

## 17.3 Document Revision Date

Month 1999 Comment

## 17.4 Document ID

LD_007_010_001_00_00_0_yyyymmdd (Release Date) *[get this from ASDC User Services]*

## 17.5 Citation

Please provide a reference to the following paper when scientific results are published using the CERES XYZ TRMM data:

"Wielicki, B. A.; Barkstrom, B.R.; Harrison, E. F.; Lee III,R.B.; Smith, G.L.; and Cooper, J.E., 1996: Clouds and the Earth's Radiant Energy System (CERES): An Earth Observing System Experiment, Bull. Amer. Meteor. Soc., 77, 853-868."

When Langley Atmospheric Sciences Data Center (ASDC) data are used in a publication, the following acknowledgment is requested to be included:

"These data were obtained from the NASA Langley Research Center EOSDIS Distributed Active Archive Center."

The Data Center at Langley requests two reprints of any published papers or reports which cite the use of data the Langley ASDC have distributed. This will help the ASDC to determine the use of data distributed, which is helpful in optimizing product development. It also helps the ASDC to keep product related references current.

## 17.6 Redistribution of Data

To assist the Langley ASDC in providing the best service to the scientific community, a notification is requested if these data are transmitted to other researchers.

## 17.7 Document Curator

The Langley ASDC Science, User & Data Services Office.

# 18.0 Index

[A], [B], [C], [D], [E], [F], [G], [H], [I], [J], [K], [L], [M], [N], [O], [P], [Q], [R], [S], [T], [U], [V], [W], [X], [Y], [Z]

## A

Acronyms, list, 16.1 . . . . . 54

ADM
definition, Note-4 . . . . . 44

Along-track scan (See azimuth scan plane, ES8-20, word 3) . . . . . 22

Angle
azimuth, ES8-8 . . . . . 16
colatitude (See Colatitude)
cone, Term-1 . . . . . 50
elevation, Term-5 . . . . . 50
longitude (See Longitude)
relative azimuth angle, ES8-8 . . . . . 16
solar zenith, ES8-7 . . . . . 16
viewing zenith, ES8-6 . . . . . 16

## B

BDRF (See ADM)

Bidirectional function (See ADM)

## C

CERES
instrument character name, Table A-1. . . . . A-1
point spread function, Note-3 . . . . . 39
satellite character name, Table A-1. . . . . A-1

Channel
SW, ES8-4 . . . . . 15
TOT, ES8-3 . . . . . 14
WN, ES8-5 . . . . . 15

Citation for data use, 17.5 . . . . . 58

Clear area (See Scene type at observation)

Cloud fraction (See Scene type at observation)

Colatitude
definition
Figure 4-1. . . . . 12
Note-2 . . . . . 38

of observation at TOA, ES8-1 . . . . . 13
of satellite, ES8-V15 . . . . . 12
of Sun, ES8-V19 . . . . . 13

Cone angle, Term-1 . . . . . 50

Count conversion, Term-2 . . . . . 50

Cross-track scan (See azimuth scan plane, ES8-20, word 3) . . . . . 22

## D

Data
granularity, 5.1 . . . . . 30
metadata, APPENDIX A . . . . . A-1
organization, 5.0 . . . . . 29
use
citation, 17.5 . . . . . 58
redistribution of data, 17.6 . . . . . 58

Default fill values, 4.4 . . . . . 28

## E

Earth
Sun distance, ES8-V2 . . . . . 10
surface model, Term-4 . . . . . 50

Elevation angle, Term-5 . . . . . 50

ERBE 12 scene types, ES8-14 . . . . . 19

ES8 header
ES8-V1 Time at observation . . . . . 9
ES8-V2 Earth-Sun distance at record start . . . . . 10
ES8-V3 X component of satellite position at record start . . . . . 10
ES8-V4 X component of satellite position at record end . . . . . 10
ES8-V5 Y component of satellite position at record start . . . . . 10
ES8-V6 Y component of satellite position at record end . . . . . 10
ES8-V7 Z component of satellite position at record start . . . . . 11
ES8-V8 Z component of satellite position at record end . . . . . 11
ES8-V9 X component of satellite velocity at record start . . . . . 11
ES8-V10 X component of satellite velocity at record end . . . . . 11
ES8-V11 Y component of satellite velocity at record start . . . . . 11
ES8-V12 Y component of satellite velocity at record end . . . . . 11
ES8-V13 Z component of satellite velocity at record start . . . . . 11
ES8-V14 Z component of satellite velocity at record end . . . . . 12
ES8-V15 Colatitude of satellite nadir at record start . . . . . 12
ES8-V16 Colatitude of satellite nadir at record end . . . . . 12
ES8-V17 Longitude of satellite nadir at record start . . . . . 12
ES8-V18 Longitude of satellite nadir at record end . . . . . 13
ES8-V19 Colatitude of Sun at observation . . . . . 13
ES8-V20 Longitude of Sun at observation . . . . . 13

ES8 parameters
ES8-1 Colatitude of CERES FOV at TOA . . . . . 13
ES8-2 Longitude of CERES FOV at TOA . . . . . 14
ES8-3 CERES TOT filtered radiance . . . . . 14
ES8-4 CERES SW filtered radiance . . . . . 15
ES8-5 CERES WN filtered radiance . . . . . 15
ES8-6 CERES viewing zenith at TOA . . . . . 16
ES8-7 CERES solar zenith at TOA . . . . . 16
ES8-8 CERES relative azimuth at TOA . . . . . 16
ES8-9 CERES SW unfiltered radiance . . . . . 16
ES8-10 CERES LW unfiltered radiance . . . . . 17
ES8-11 CERES WN unfiltered radiance . . . . . 18
ES8-12 CERES SW flux at TOA . . . . . 18
ES8-13 CERES LW flux at TOA . . . . . 19
ES8-14 ERBE scene identification at observation . . . . . 19
ES8-15 TOT channel flag words . . . . . 20
ES8-16 SW channel flag words . . . . . 21
ES8-17 WN channel flag words . . . . . 21
ES8-18 Scanner FOV flag words . . . . . 21
ES8-19 Rapid retrace flag words . . . . . 22
ES8-20 Scanner operations flag word . . . . . 22

ES8 production data and time, Table A-2. . . . . A-3

## F

FAPS (See Fixed azimuth plane scan)

Fast return or retrace, Term-13 . . . . . 51

Field of view
colatitude at TOA, ES8-1 . . . . . 13
definition, Term-5 . . . . . 50
flag, quality ES8-18 . . . . . 21
longitude at TOA, ES8-2 . . . . . 14

Fill values, 4.4 . . . . . 28

Filtered radiance (See Radiance)

Fixed azimuth plane scan (FAPS)
definition, Term-7 . . . . . 51
flag, ES8-20, word 3 . . . . . 22

Flags
azimuth motion status, ES8-20, word 1 . . . . . 22
azimuth scan plane, ES8-20, word 2, word 3 . . . . . 22
elevation motor status, ES8-20, word 1 . . . . . 22
elevation scan profile, ES8-20, word 2 . . . . . 22
FOV, ES8-18 . . . . . 21
Instrument mode, ES8-20, word 1 . . . . . 22
Internal calibration status, ES8-20, word 1 . . . . . 22
radiance

SW, ES8-16 . . . . . 21
TOT, ES8-15 . . . . . 20
WN, ES8-17 . . . . . 21
rapid retrace, ES8-19 . . . . . 22
scanner operations, ES8-20 . . . . . 22
SWICS status, ES8-20, word 1 . . . . . 22

Flux
LW at TOA, ES8-13 . . . . . 19
SW at TOA, ES8-12 . . . . . 18

FOV (See Field of view)

## G

Geocentric Colatitude definition, Term-8 . . . . . 51

Glossary of Terms, 15.0 . . . . . 50

Granule, 5.1 . . . . . 30

Granule, Term-9 . . . . . 51

Greenwich
coordinate system definition, Term-3 . . . . . 50
Julian Date, (See Julian Date)

## H

Header (See ES8 header)

## I

Identification
character name of CERES instrument, Table A-1. . . . . A-1
character name of satellite, Table A-1. . . . . A-1
ES8 data product, Table A-2. . . . . A-3
IES data used as input, Table A-2. . . . . A-3

Instrument character name, Table A-1. . . . . A-1

## J

Julian date
definition
Note-1 . . . . . 35
Term-10 . . . . . 51
table, Table 8-1 . . . . . 37
time of observation, ES8-V1 . . . . . 9

## L

Latitude (See Colatitude)

Limbdarkening (See ADM)

Longitude
- definition
  - Figure 4-1. . . . . 12
  - Note-2 . . . . . 38
- of observation at TOA, ES8-2 . . . . . 14
- of satellite, ES8-V17 . . . . . 12
- of Sun, ES8-V20 . . . . . 13

Longwave (LW)
- channel (See Total channel)
- flux at TOA, ES8-13 . . . . . 19
- unfiltered radiance, ES8-10 . . . . . 17

## M

Maximum likelihood estimator, Note-5 . . . . . 45

Measurement (See Observation)

MLE (See Maximum likelihood estimator), 18.0

## N

Nadir
- colatitude, ES8-15 . . . . . 20
- definition
  - Note-2 . . . . . 38
  - Term-11 . . . . . 51
- longitude, ES8-17 . . . . . 21

North pole definition, Term-3 . . . . . 50

Notes
- Note-1 Conversion of Julian Date to Calendar Date . . . . . 35
- Note-2 Colatitude and Longitude of Nadir . . . . . 38
- Note-3 CERES Point Spread Function . . . . . 39
- Note-4 Definition of Angular Distribution Models (ADM) . . . . . 44
- Note-5 Maximum Likelihood Estimator (MLE) of Scene Type . . . . . 45
- Note-6 Spectral Correction Algorithm . . . . . 46

## O

Observation
- colatitude at TOA, ES8-1 . . . . . 13
- longitude at TOA, ES8-2 . . . . . 14
- radiance (See Radiance)

scene identification, ES8-14 . . . . . 19
time, ES8-V1 . . . . . 9

Operation flag, ES8-20 . . . . . 22

## P

Point Spread Function (PSF)
definition,Term-12 . . . . . 51
model, Note-3 . . . . . 39

Position
of observation
colatitude, ES8-1 . . . . . 13
longitude, ES8-2 . . . . . 14
of satellite
colatitude
ES8-V15 . . . . . 12
Note-2 . . . . . 38
longitude
ES8-V17 . . . . . 12
Note-2 . . . . . 38
XYZ, ES8-V3 . . . . . 10
of Sun
colatitude ,ES8-V19 . . . . . 13
longitude, ES8-V20 . . . . . 13

PSF (See Point Spread Function)

## R

Radiance
filtered
SW, ES8-4 . . . . . 15
TOT, ES8-3 . . . . . 14
WN, ES8-5 . . . . . 15
flags, quality
SW, ES8-16 . . . . . 21
TOT, ES8-15 . . . . . 20
WN, ES8-17 . . . . . 21
unfiltered
LW, ES8-10 . . . . . 17
SW, ES8-9 . . . . . 16
WN, ES8-11 . . . . . 18

Radiant exitance (See Flux)

Rapid retrace flag, ES8-19 . . . . . 22

Rapid retrace, Term-13 . . . . . 51

RAPS (See Rotating azimuth plane scan)

Record, Term-14 . . . . . 52

References, 14.0 . . . . . 49

Relative azimuth angle, ES8-8 . . . . . 16

Resolution
definition, Term-15 . . . . . 52
spatial, 4.1.2 . . . . . 8
temporal, 4.2.2 . . . . . 9

Rotating azimuth plane scan (RAPS)
definition, Term-16 . . . . . 52
flag, ES8-20, word 3 . . . . . 22

## S

Satellite
character name, Table A-1. . . . . A-1
colatitude
ES8-V15 . . . . . 12
Note-2 . . . . . 38
cone angle, Term-1 . . . . . 50
longitude
ES8-V17 . . . . . 12
Note-2 . . . . . 38
nadir, Note-2 . . . . . 38
XYZ position, ES8-3 . . . . . 14
XYZ velocity, ES8-9 . . . . . 16

Scan
cycle, Term-17 . . . . . 52
sample number, Term-18 . . . . . 52

Scanner operations flag, ES8-20 . . . . . 22

Scene type at observation, ES8-14 . . . . . 19

Science Data Set (SDS), Term-19 . . . . . 53

Shortwave (SW) channel
filtered radiance, ES8-4 . . . . . 15
flags, radiance quality, ES8-16 . . . . . 21
flux at TOA, ES8-12 . . . . . 18
unfiltered radiance, ES8-9 . . . . . 16

Solar zenith angle, ES8-7 . . . . . 16

Spacecraft (See Satellite)

Spectral correction
algorithm, Note-6 . . . . . 46
definition, Term-20 . . . . . 53

Subsatellite point (See Nadir)

Subsolar point, Term-21 . . . . . 53

Sun
colatitude, ES8-V19 . . . . . 13
earth distance at, ES8-V2 . . . . . 10
longitude, ES8-V20 . . . . . 13
solar zenith angle, ES8-7 . . . . . 16

Surface model of Earth, Term-4 . . . . . 50

## T

Terms, 15.0 . . . . . 50

Time
and date of ES8 product, Table A-2. . . . . A-3
of observation, ES8-V1 . . . . . 9

TOA (See Top of atmosphere)

Top of atmosphere
Angles
azimuth, ES8-8 . . . . . 16
colatitude of observation, ES8-1 . . . . . 13
longitude of observation, ES8-2 . . . . . 14
relative azimuth angle, ES8-8 . . . . . 16
solar zenith, ES8-7 . . . . . 16
viewing zenith, ES8-6 . . . . . 16
Flux
LW, ES8-13 . . . . . 19
SW, ES8-12 . . . . . 18
model, Term-21 . . . . . 53
Scene identification, ES8-14 . . . . . 19
TOA point definition, Term-22 . . . . . 53

Total (TOT) channel
filtered radiance, ES8-3 . . . . . 14
flag, radiance quality, ES8-15 . . . . . 20

## U

Unfiltered radiance (See Radiance)

Units, definitions, 16.2 . . . . . 56

## V

Vdata
list of parameters, Table 5-4 . . . . . 31

Viewing zenith angle, ES8-6 . . . . . 16

## W

Window (WN) channel
filtered radiance, ES8-5 . . . . . 15
flag, radiance quality, ES8-17 . . . . . 21
unfiltered radiance, ES8-11 . . . . . 18

## X

XYZ
components of satellite position, ES8-V3 . . . . . 10
components of satellity velocity, ES8-V9 . . . . . 11

## Z

Zenith
solar angle, ES8-7 . . . . . 16
viewing angle, ES8-6 . . . . . 16

# APPENDIX A
# CERES Metadata

This section describes the metadata that are written to all CERES HDF products. Table A-1 describes the CERES Baseline Header Metadata that are written on both HDF and binary direct access output science data products. The parameters are written in HDF structures for CERES HDF output products and are written as 80-byte records for binary direct access output products. Some parameters may be written in multiple records. Table A-2 describes the CERES_metadata Vdata parameters which are a subset of the CERES Baseline Header Metadata and are also written to all CERES HDF output products. For details on CERES Metadata, see the CERES Software Bulletin "CERES Metadata Requirements for LaTIS" (Reference 11).

Table A-1 lists the item number, parameter name, units, range or allowable values, the data type, and the maximum number of elements. Note that there are two choices for parameters 22-25 and two choices for parameters 26-29. The choices depend on whether the product is described by a bounding rectangle or by a GRing. Abbreviations used in the Data Type field are defined as:

| | | |
|---|---|---|
| s = string | date = | yyyy-mm-dd |
| F = float | time = | hh:mm:ss.xxxxxxZ |
| I = integer | datetime = | yyyy-mm-ddThh:mm:ss.xxxxxxZ |

Table A-1. CERES Baseline Header Metadata (1 of 3)

| Item | Parameter Name | Units | Range | Data Type | No. of Elements |
|---|---|---|---|---|---|
| 1 | ShortName | N/A | N/A | s(8) | 1 |
| 2 | VersionID | N/A | 0 .. 255 | I3 | 1 |
| 3 | CERPGEName | N/A | N/A | s(20) | 1 |
| 4 | SamplingStrategy | N/A | CERES, TRMM-PFM-VIRS, Terra-FM1-MODIS, TBD | s(20) | 1 |
| 5 | ProductionStrategy | N/A | Edition, Campaign, Diagnostic-Case, PreFlight, TBD | s(20) | 1 |
| 6 | CERDataDateYear | N/A | 1997 .. 2050 | s(4) | 1 |
| 7 | CERDataDateMonth | N/A | 1 .. 12 | s(2) | 1 |
| 8 | CERDataDateDay | N/A | 1 .. 31 | s(2) | 1 |
| 9 | CERHrOfMonth | N/A | 1 .. 744 | s(3) | 1 |
| 10 | RangeBeginningDate | N/A | 1997-11-19 .. 2050-12-31 | date | 1 |
| 11 | RangeBeginningTime | N/A | 00:00:00.000000Z .. 24:00:00:000000Z | time | 1 |
| 12 | RangeEndingDate | N/A | 1997-11-19 .. 2050-12-31 | date | 1 |
| 13 | RangeEndingTime | N/A | 00:00:00.000000Z .. 24:00:00:000000Z | time | 1 |

Table A-1. CERES Baseline Header Metadata (2 of 3)

| Item | Parameter Name | Units | Range | Data Type | No. of Elements |
|---|---|---|---|---|---|
| 14 | AssociatedPlatformShortName | N/A | TRMM, Terra, Aqua, TBD | s(20) | 1-4 |
| 15 | AssociatedInstrumentShortName | N/A | PFM, FM1, FM2, FM3, FM4, FM5, TBD | s(20) | 1-4 |
| 16 | LocalGranuleID | N/A | N/A | s(80) | 1 |
| 17 | PGEVersion | N/A | N/A | s(10) | 1 |
| 18 | CERProductionDateTime | N/A | N/A | datetime | 1 |
| 19 | LocalVersionID | N/A | N/A | s(60) | 1 |
| 20 | ProductGenerationLOC | N/A | SGI_xxx, TBD | s(255) | 1 |
| 21 | NumberofRecords | N/A | 1 .. 9 999 999 999 | I10 | 1 |
| 22 | WestBoundingCoordinate | deg | -180.0 .. 180.0 | F11.6 | 1 |
| 23 | NorthBoundingCoordinate | deg | -90.0 .. 90.0 | F11.6 | 1 |
| 24 | EastBoundingCoordinate | deg | -180.0 .. 180.0 | F11.6 | 1 |
| 25 | SouthBoundingCoordinate | deg | -90.0 .. 90.0 | F11.6 | 1 |
| 22 | GRingPointLatitude | deg | -90.0 .. 90.0 | F11.6 | 5 |
| 23 | GRingPointLongitude | deg | -180.0 .. 180.0 | F11.6 | 5 |
| 24 | GRingPointSequenceNo | N/A | 0 .. 99999 | I5 | 5 |
| 25 | ExclusionGRingFlag | N/A | Y (= YES), N (= NO) | s(1) | 1 |
| 26 | CERWestBoundingCoordinate | deg | 0.0 .. 360.0 | F11.6 | 1 |
| 27 | CERNorthBoundingCoordinate | deg | 0.0 .. 180.0 | F11.6 | 1 |
| 28 | CEREastBoundingCoordinate | deg | 0.0 .. 360.0 | F11.6 | 1 |
| 29 | CERSouthBoundingCoordinate | deg | 0.0 .. 180.0 | F11.6 | 1 |
| 26 | CERGRingPointLatitude | deg | 0.0 .. 180.0 | F11.6 | 5 |
| 27 | CERGRingPointLongitude | deg | 0.0 .. 360.0 | F11.6 | 5 |
| 28 | GRingPointSequenceNo | N/A | 0 .. 99999 | I5 | 5 |
| 29 | ExclusionGRingFlag | N/A | Y (= YES), N (= NO) | s(1) | 1 |
| 30 | AutomaticQualityFlag | N/A | Passed, Failed, or Suspect | s(64) | 1 |
| 31 | AutomaticQualityFlagExplanation | N/A | N/A | s(255) | 1 |
| 32 | QAGranuleFilename | N/A | N/A | s(255) | 1 |
| 33 | ValidationFilename | N/A | N/A | s(255) | 1 |
| 34 | ImagerShortName | N/A | VIRS, MODIS, TBD | s(20) | 1 |
| 35 | InputPointer | N/A | N/A | s(255) | 800 |

Table A-1. CERES Baseline Header Metadata (3 of 3)

| Item | Parameter Name | Units | Range | Data Type | No. of Elements |
|---|---|---|---|---|---|
| 36 | NumberInputFiles | N/A | 1 .. 9999 | I4 | 1 |

Table A-2 describes the CERES_metadata Vdata parameters which are written to all CERES HDF output science products. The table lists the item number, parameter name, units, range or allowable values, and the parameter data type where s(x) denotes a string of x characters.

Table A-2. CERES_metadata Vdata

| Item | Parameter Name | Units | Range | Data Type |
|---|---|---|---|---|
| 1 | ShortName | N/A | N/A | s(32) |
| 2 | RangeBeginningDate | N/A | 1997-11-19 .. 2050-12-31 | s(32) |
| 3 | RangeBeginningTime | N/A | 00:00:00.000000Z .. 24:00:00:000000Z | s(32) |
| 4 | RangeEndingDate | N/A | 1997-11-19 .. 2050-12-31 | s(32) |
| 5 | RangeEndingTime | N/A | 00:00:00.000000Z .. 24:00:00:000000Z | s(32) |
| 6 | AutomaticQualityFlag | N/A | Passed, Failed, or Suspect | s(64) |
| 7 | AutomaticQualityFlagExplanation | N/A | N/A | s(256) |
| 8 | AssociatedPlatformShortName | N/A | TRMM, Terra, Aqua, TBD | s(32) |
| 9 | AssociatedInstrumentShortName | N/A | PFM, FM1, FM2, FM3, FM4, FM5, TBD | s(32) |
| 10 | LocalGranuleID | N/A | N/A | s(96) |
| 11 | LocalVersionID | N/A | N/A | s(64) |
| 12 | CERProductionDateTime | N/A | N/A | s(32) |
| 13 | NumberofRecords | N/A | 1 .. 9 999 999 999 | 4-byte integer |
| 14 | ProductGenerationLOC | N/A | SGI_xxx, TBD | s(256) |